Scots Pine (*Pinus sylvestris* L.) Sapwood Modification by Vinyl Acetate–Epoxidized Plant Oil Copolymer

Precursor Syntheses, Characterization, Modified Wood Properties and Durability

Shengzhen Cai

Faculty of Forest Sciences
Department of Forest Products
Uppsala

Doctoral Thesis
Swedish University of Agricultural Sciences
Uppsala 2016

Acta Universitatis agriculturae Sueciae

2016:126

Scots Pine (*Pinus sylvestris* L.) Sapwood Modification by Vinyl Acetate–Epoxidized Plant Oil Copolymer. Precursor Syntheses, Characterization, Modified Wood Properties and Durability

Abstract

A new bio-based formulation consisting of plant oil and vinyl acetate was developed for wood modification aiming at improving some of the material's properties. *In–situ* epoxidation of linseed oil (LO) and soybean oil (SO) was carried out at different times with purpose of preparing epoxidized oils with various epoxy content. For comparison, commercially available epoxidized linseed oil (ELO®) and epoxidized soybean oil (ESO®) were also included in the study. The epoxidized oils were subsequently reacted with vinyl acetate (VAc) to investigate the effect of epoxidation degree on the copolymerization reaction between epoxidized oils and VAc. Results showed that a copolymer can be formed between VAc and epoxidized LO with high epoxy content, while no reaction occurred between VAc and SO or its epoxidized derivatives. As the most reactive monomer among studied oils, the epoxidized LO with highest epoxy content (*i.e.* ELO®) was selected for further investigation to determine the optimal conditions for its copolymerization reaction with VAc. The effect of feed ratio, reaction temperature, reaction time and catalyst amount on the efficiency of the copolymerization reaction was evaluated by measuring the yields of formed copolymer under different conditions. DSC and NMR were used to confirm the formation of copolymer and reveal the chemical structure of the obtained copolymer.

The optimized formulation was further impregnated into wood and subsequently cured, and the progress of curing process monitored using ATR–FTIR spectroscopy. It was found that an increase of curing temperature or duration resulted in improved wood dimensional stability, while weight percentage gain (WPG) was not significantly affected. In addition, insignificant correlation between WPG and anti–swelling efficiency (ASE) was found for the VAc–ELO® treated wood. From energy saving and economical point of view, 168 h of curing duration at 90°C is sufficient to achieve a satisfying dimensional stability. Moreover, the VAc–ELO® treated wood showed great leaching resistance to water. By using light– and scanning electron microscopy, it was found that the copolymer formed inside wood was mainly located in rays, resin canals and occasionally in the cell lumina. Like most wood treatments, the mechanical properties of VAc–ELO® treated wood samples were slightly decreased compared to untreated wood, especially MOR, compression parallel to the grain (∥) and hardness perpendicular to the grain (⊥). The difference between control and treated samples gradually increase as a result of increasing WPG. Durability tests showed that 8% WPG was enough to ensure decay resistance against the tested fungi (improved up to

durability class 2), and thus can be used to protect wood used in above ground applications.

Author's address: Shengzhen Cai, SLU, Department of Forest Products,
P.O. Box 7008, 750 07 Uppsala, Sweden
E–mail: shengzhen.cai@slu.se

Dedication

To the members of my family for their continued love and support.

In the end, it's not the years in your life that count. It's the life in your years.
   Abraham Lincoln

Contents

List of Publications

This thesis is based on the work contained in the following papers:

I Jebrane, M., Cai, S., Panov, D., Yang, X. & Terziev, N. (2015). Synthesis and characterization of new vinyl acetate grafting onto epoxidized linseed oil in aqueous media. *Journal of applied polymer science,* 132(24), pp. 42089.

II Cai, S., Jebrane, M. & Terziev, N. (2016). Curing of wood treated with vinyl acetate–epoxidized linseed oil copolymer (VAc–ELO). *Holzforschung,* 70(4), pp. 305–312.

III Cai, S., Jebrane, M., Terziev, N. & Daniel, G. (2016). Mechanical properties and decay resistance of Scots pine (Pinus sylvestris L.) sapwood modified by vinyl acetate–epoxidized linseed oil copolymer. *Holzforschung*, 70(9), pp. 885–894.

IV Cai, S., Jebrane, M., & Terziev, N. (2014). Properties of epoxidized linseed oil–furfuryl alcohol & vinyl acetate–furfuryl alcohol treated wood. *Proceedings of the 10th meeting of the northern European network for wood science and engineering*, Edinburgh, Scotland, 13–14 October 2014.

V Jebrane, M., Cai, S., Sandström, C., & Terziev, N. (2016). The reactivity of linseed and soybean oil with various epoxidation degree towards vinyl acetate and impact of the resulting copolymer on the wood durability (submitted to *Express Polymer Letters*).

Papers I–IV are reproduced with the permission of the publishers

The contribution of Shengzhen Cai to the papers included in this thesis was as follows:

I Cai, S. has participated in the design of the experiments, carried out the analytical and practical work. (60% of the total contribution)

II Cai, S. has participated in the design of the experiment, planning and carried out the experimental work on curing parameters. (70% of the total contribution)

III Cai, S. has participated in the design of the experiments and carried out the entire mechanical testing of the treated wood. (70% of the total contribution)

IV Cai, S. has participated in the design of the experiments, carried out the mechanical tests and presented the study at the conference in Scotland. (60% of the total contribution)

V Cai, S. has participated in the design of the experiments, carried out the chemical synthesis of the co–polymers. (60% of the total contribution)

Abbreviations

AA	acetic acid
AESO	acrylated epoxidized soybean oil
ASE	anti–swelling efficiency
ATR–FTIR	attenuated total reflectance FTIR
Brij® S 100	polyoxyethylene stearyl ether
CTAB	cetyltrimethylammonium bromide
DC	durability class
DMDHEU	1,3–dimethylol–4,5–dihydroxyethylene urea
DOE	degree of epoxidation
DSC	differential scanning calorimetry
ELO®	commercial epoxidized linseed oil
EMC	equilibrium moisture content
ELO®	commercial epoxidized soybean oil
FA	furfuryl alcohol
FSP	fibre saturation point
FTIR	Fourier Transform Infrared Spectroscopy
IV	iodine value
LO	linseed oil
MC	moisture content
ML	mass loss
MOE	modulus of elasticity
MOR	modulus of rupture
NMR	nuclear magnetic resonance
PEG	polyethylene glycol
PVA	polyvinyl alcohol
PVAc	polyvinyl acetate
RH	relative humidity
SEM	scanning electron microscopy
Span® 80	sorbitane monooleate

SO	soybean oil
T_g	glass transition temperature
TO	tung oil
VAc	vinyl acetate
WPG	weight percentage gain
WS–OD	water soaking and oven drying
‖	parallel
⊥	perpendicular

1   Introduction

1.1   Plant oils and their derivatives

Due to the public's growing environmental awareness, the utilization of natural products is attracting considerable interests. Plant oils are extracted from naturally–occurring raw materials and used widely in the chemical industry. Due to their ready availability, renewability, biodegradability, low volatility and low toxicity, plant oils are extensively used for the production of coatings, inks, plasticizers, lubricants, agrochemicals, etc. (Sharma & Kundu, 2006).

The plant oils are triglyceride molecules that combine glycerol with fatty acid chains of different unsaturation degree. The structures of oils' common fatty acids are illustrated in Figure 1. The degree of unsaturation can be reflected by the iodine value (IV) which is defined as the grams of iodine consumed by 100 g oil. Depending on IV, the plant oils can be classified into three types, *i.e.* drying (IV≥170), semi–drying (170>IV≥100) and non–drying oils (IV<100) (Meier *et al*., 2007). The plant oils are usually named according to their biological source. Linseed oil (LO) derived from the seeds of flax plant (*Linum usitatissimum*) is a typical drying oil, which contains approximately 57% α–linolenic acid (Xia & Larock, 2010). Soybean oil (SO) extracted from the seeds of the soybean (*Glycine max*) is composed of 54% linoleic acid, which is regarded as semi–drying oil (Xia & Larock, 2010).
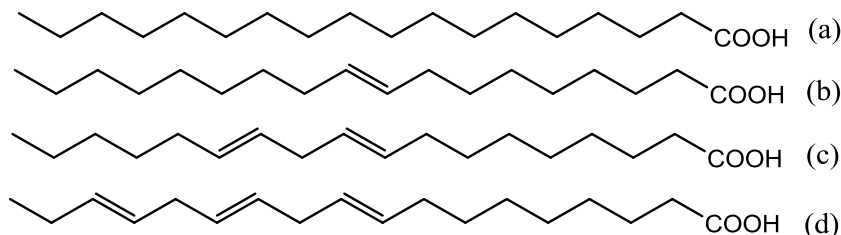

Figure 1. Structure of stearic (a), oleic (b), linoleic (c), and linolenic (d) acid.

As renewable resources, the plant oils can be used as alternatives to the petroleum–based chemicals for the production of resin and polymeric materials. The reactivity of unmodified plant oil is attributed to the esters and double bonds in triglyceride. The transesterification by alcoholysis or acidolysis can proceed at esters of the triglycerides (Schuchardt *et al.*, 1998), while the double bonds can undergo cationic or radical copolymerization with a variety of vinyl monomers or through auto–oxidation with other triglycerides (Meier *et al.*, 2007; Schuchardt *et al.*, 1998). Previous studies reported cationic copolymerization of SO, corn or tung oil (TO) with vinyl monomers (Li *et al.*, 2003; Li *et al.*, 2001; Li & Larock, 2001; Li & Larock, 2000). Depending on the stoichiometry of the plant oils and the types of vinyl monomers used, copolymers ranging from elastomers to tough and rigid plastics can be obtained, which exhibit a wide range of thermal and mechanical properties. For radical copolymerization, TO composed of 84% α–eleostearic acid (characterized by conjugated double bonds) can radical copolymerize with divinylbenzene and styrene initiated by free radicals produced either by heating styrene or by adding initiator, such as tert–butyl hydroperoxide (TBHP) or benzoyl peroxide (Li & Larock, 2003). Alternatively, the LO or SO can be converted to conjugated LO or SO in the presence of rhodium–based catalysts with the purpose of making it more reactive (Larock *et al.*, 2001). Non–conjugated plant oils, however, are less reactive and cannot be readily initiated by radicals.

As most of the double bonds in oils are insufficiently active for radical polymerization, the reactivity can be chemically improved by converting double bonds into more reactive groups, such as epoxy, hydroxyl, acrylate, carboxyl groups, etc. (Saithai *et al.*, 2013; Guo *et al.*, 2000). The epoxidized plant oils can be chemically produced from the corresponding plant oil by *in–situ* epoxidation with hydrogen peroxide and acetic acid (AA) in the presence of sulfuric acid as catalyst (Saithai *et al.*, 2013; Saurabh *et al.*, 2011). The process of epoxidation reaction can be generally considered in two steps, the formation of peracetic acid and the following reaction of peracetic acid with double bonds (Figure 2). However, the presence of strong acid can adversely catalyse ring–opening of the formed oxirane by protonation. As an alternative to *in–situ* epoxidation, a chemo–enzymatic synthesis of epoxidized plant oil catalyzed by lipase has also been developed (Warwel, 1999). Compared to the chemo–enzymatic method, *in–situ* epoxidation by peroxy acid is by far more convenient and economically viable in industry (Saithai *et al.*, 2013; Xia & Larock, 2010).

$$\text{RCOOH} \; + \; \text{H}_2\text{O}_2 \; \underset{}{\overset{\text{H}^+}{\rightleftharpoons}} \; \text{RCOOOH} \; + \; \text{H}_2\text{O}$$

$$\text{RCOOOH} \; + \; \text{R}-\text{CH}=\text{CH}-\text{R}' \; \longrightarrow \; \text{R}-\text{CH}\underset{\text{O}}{\overset{}{-}}\text{CH}-\text{R}'$$
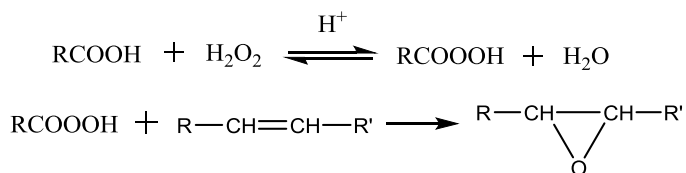
Figure 2. General plant oil epoxidation procedure

The epoxidized plant oil can be further functionalized by ring–opening of the formed epoxy groups. The epoxide groups in plant oil can be polymerized by anionic or cationic polymerization. Anionic polymerization can be initiated by metal hydroxides, alkoxides, oxides, amides, metal alkyls, aryls, etc. (Odian, 2004). Regarding cationic polymerization, the oxygen atom of the epoxy group is protonated into oxonium ion which makes the α–carbon atom of the oxonium ion rather electron–deficient. The electron–deficient carbon atom facilitates the attack by another epoxide monomer. Both protonic acids, such as trifluoroacetic and trifluoromethanesulfonic acid, and Lewis acids can be used to initiate cationic polymerization (Odian, 2004). Lewis acids, such as BF_3 and $SbCl_5$, can combine with protogen or cationogen to initiate polymerization of cyclic ethers. The formation of initiator–co–initiator complex proceeds to provide proton or carbocation to initiate ring opening reaction of epoxide monomer at increased temperatures (Odian, 2004).

Copolymers of epoxidized plant oil with other monomer(s) have been studied extensively, aiming at achieving desirable thermal, physical and mechanical properties. The acrylated epoxidized soybean oil (AESO) obtained by ring–opening of epoxidized soybean oil (ESO) with acrylic acid can be further crosslinked with divinylbenzene (DVB) or phthalic anhydride obtaining resin with increased T_g (Zhan & Wool, 2010). Moreover, there is a vast array of literature studying polyurethane (PU) synthesized by isocyanate and polyols derived from ring opening of epoxidized plant oils (Grishchuk & Karger–Kocsis, 2011; Petrović, 2008; Zlatanić *et al.*, 2004). Recently, Clark et al. (2014) studied the copolymerization of tetrahydrofuran and epoxidized plant oil initiated by the strong Lewis acid $BF_3 \cdot OEt_2$.

1.2 Wood modification by plant oils

1.2.1 Definition of wood modification

As a natural renewable resource, wood is a non–toxic, easily accessible and inexpensive biomass–derived material that has continuously attracted people's attention throughout mankind's history. Wood is used in civil and furniture construction, paper and pulp manufacturing, and as fuel to give energy.

Structurally, wood is a porous, hygroscopic and anisotropic biopolymer composite which consists mostly of cellulose, hemicellulose and lignin (Rowell, 2012). The hydroxyl groups of cellulose, hemicellulose and lignin are considered as the most reactive sites in wood, and most wood modification schemes are associated with the reaction of these hydroxyl groups. At the same time, the hydroxyl groups allow equilibrate the wood moisture with the moisture of the surrounding environment. There are two main forms of water in wood: bound water attached to the cell walls and free water presented in the cell cavities (lumina). The moisture content (MC) at which all of the free water is removed while maximum amount of bound water is held by the wood is defined as the fibre saturation point (FSP). When wood is exposed to moisture, the water molecules are progressively transported into the cell wall and some of them are bonded to the cell wall polymer through hydrogen bonding. Wood swells proportionally to the moisture adsorbed until the FSP is reached. Any additional moisture absorbed can only be deposited in the cell lumen or cell wall cavities, acting as free water which cannot cause further wood swelling. Apart from the influence of FSP on the changes of wood dimensions, the FSP is also associated with susceptibility of wood to fungal attack, and mechanical behaviour of wood. The changes in mechanical properties are associated with the changes of the bound water, which only occur when the MC of wood is below FSP. Additionally, as a decisive factor for wood degradation, decay fungi can cause serious damage when the MC is above the FSP. High MC promotes the degradation of wood cell wall by the enzymes generated by fungi (Gamauf *et al.*, 2007; Nicholas, 1982).

Although biomass–derived wood has been extensively used in many areas, the negative aspects of wood cannot be avoided. Most of the untreated wood products suffer problems of flammability, dimensional instability, UV degradation and low resistance to decay fungi, which limits the application of wood in service. However, the properties of wood can be improved by wood modification which can be generally categorized into chemical modification and non–chemical modification. According to Rowell (Rowell, 2005), chemical modification is defined as:

"*A chemical reaction between some reactive part of wood and a simple single chemical reagent, with or without catalyst, to form a covalent bond between the two.*"

While those treatments do not form covalent bonds with cell wall polymers are collectively termed as "non–chemical modification".

Chemical modification

A covalent bond is formed between wood and impregnating agent by reaction between the chemical reagent (such as anhydrides, epoxides and isocyanates) and the hydrophilic hydroxyl group of wood cell wall polymers. The reduced number of hydroxyl groups permanently render wood more hydrophobic, dimensionally stable and durable against decay fungi. There is a considerable literature on the various methods for the wood chemical modification (Rowell, 2005). Some of these methods have already been commercialized, such as the acetylation, furfurylation and the application of 1,3–dimethylol–4,5–dihydroxyethylene urea (DMDHEU) (Militz & Lande, 2009).

Acetylated wood can be formed by reacting wood with acetic anhydride, acetyl chlorides, thioacetic acid, and ketene (Jebrane *et al.*, 2011; Hill, 2007; Kumar *et al.*, 1991). Wood acetylation by acetic anhydride is the most popular method and the resulting products have already been commercialized since 2007 (Jebrane *et al.*, 2011). Acetylated wood shows improved dimensional stability, fungal resistance, photostability and good resistance to weathering (Jebrane *et al.*, 2011). Acetylation can be carried out with or without catalysts and co–solvents (Li *et al.*, 2009; Jebrane & Sebe, 2007). Catalysts such as pyridine, potassium acetate, iodine, 4–dimethylamino pyridine, N–methyl pyrolidine, dimethyl formamide, zinc chloride, magnesium chloride hexahydrate are used in wood acetylation with acetic anhydride to increase reaction rate (Eranna & Pandey, 2012; Li *et al.*, 2009). The by–product acetic acid (AA) should be removed together with the unreacted acetic anhydride after reaction. Recently, wood acetylated by vinyl acetate (VAc) has received increasing attention, since the produced by–product acetaldehyde is non–acidic and volatile which can be readily removed after reaction (Jebrane & Sebe, 2007). Regarding wood furfurylation, furfuryl alcohol (FA) is derived from furfural which is obtained from acid hydrolysis of the pentosan contained in woody biomass (Win, 2005). Preliminary work on furfurylation of wood dates back to the early 1950s when zinc chloride was introduced as a catalyst to initiate the polymerization of FA (Goldstein, 1955). In the early 1990s, Schneider (1995) proposed utilization of cyclic carboxylic anhydrides as catalysts. The cyclic carboxylic anhydrides (mainly maleic anhydride) are soluble in FA and the resulting solutions are stable with no significant harmful effects towards the environment (Pilgård *et al.*, 2010; Lande *et al.*, 2004a). According to nuclear magnetic resonance (NMR) studies, it was presumed that the aromatic lignin units containing hydroxyl groups are highly reactive towards the polymerising poly(furfuryl alcohol) chains (Nordstierna *et al.*, 2008). Furfurylated wood shows reduced equilibrium moisture content (EMC) and improved dimensional stability (Epmeier *et al.*, 2004; Lande *et al.*, 2004b).

Increased hardness and significant reduced impact bending strength were observed while no obvious change was recorded for the dynamic modulus of elasticity (MOE) (Epmeier *et al.*, 2007; Lande *et al.*, 2004b).

Cross–linking of wood cell wall polymers by reaction with formaldehyde in presence of catalyst was also reported by researchers, resulting in reduction in EMC and improvement in dimensional stability (Rowell, 2012; Yasuda & Minato, 1994). The crosslinking takes place by reacting one molecule of chemical agent with two hydroxyl groups in the cell wall. Therefore the wood cell wall polymers are "locked" in a rigid structure, which does not allow the cell wall to expand much when water is adsorbed (Rowell, 2012). However, due to potential health problems that can be caused by formaldehyde vapour, efforts have been made to explore non–formaldehyde cross–linking chemicals, such as DMDHEU. The covalent cross–linking between DMDHEU and cell wall polymers has been confirmed by Fourier Transform Infrared Spectroscopy (FTIR) investigation (Yuan *et al.*, 2013). Various catalysts have been used to enhance the chemical cross–linking, e.g. $AlCl_3$, $MgCl_2$, methanesulfonic acid, citric acid, etc (Yuan *et al.*, 2013; Hill, 2007). Wood modified with DMDHEU exhibits improved dimensional stability, and resistance to decay and weathering (Yuan *et al.*, 2013; Hill, 2007). Like most of the wood treatment, reduction in strength caused by the DMDHEU was observed, depending on the catalyst used and reaction temperatures (Yuan *et al.*, 2013).

Non–chemical modification

In the cases of non–chemical modification, the impregnated agents present mainly in the cell lumen and intercellular spaces, which are not chemically bound with the wood cell wall. The leachability in water of the various impregnating agents intended for non–chemical modification is also different. Polyethylene glycol (PEG) can be impregnated into wood by diffusion. Since water soluble PEG is prone to be leached by water, the obtained products is suggested to be used for dry applications. High leachability of the impregnating agents can be prevented by finishing with a surface coating to seal the PEG in wood. PEG–impregnated wood can reduce occurrence of checks, which is suggested to apply in artistic and furniture grade lumber products (Robinson e*t al.*, 2011).

However, wood modification with thermosetting resins is normally non–leachable, such as melamine formaldehyde (MF) and phenol formaldehyde (PF). Resin–forming monomers in aqueous solution are impregnated into wood and then cured to form an insoluble polymer bulked in the cell wall with no chemical bonding between the formed resin and the cell wall components. Resin treatment showed increased dimensional stability, MOE, modulus of

rupture (MOR), hardness and compression strength perpendicular to the grain (Hill, 2007; Deka & Saikia, 2000).

Thermal modification

Apart from modification by chemical impregnation, wood of improved stability and durability can also be obtained by thermal modification without incorporation of any impregnating agents. The process of thermal degradation of cell wall polymers starts at approximately 100°C and its intensity rises with increasing temperature and duration of the treatment (Kollmann & Fengel, 1965). Thermal modification of wood always results in some mass loss (ML). Hemicellulose is the first structural compound to be thermally degraded, followed by cellulose (Rowell, 2005). The deacetylation of hemicellulose produces AA, which can further catalyse the decomposition of polysaccharides. Compared to hemicellulose, cellulose is more resistant to thermal modification due to the linear chain and intrinsic nature of the crystalline part in the cellulose. Besides changes of the carbohydrates, thermal treatments of wood also cause partial modification of lignin and extractives (Windeisen *et al.*, 2009; Boonstra *et al.*, 2007). Moreover, thermal modified wood shows decreased EMC which can be explained by the chemical change with a decrease of hydroxyl groups, decreased accessibility of hydroxyl groups to water molecules due to the increased cellulose crystallinity, and further cross–linking of lignin due to polycondensation reactions (Esteves & Pereira, 2008). However, the degradation of hemicellulose contributes to loss of a number of mechanical properties, and the degradation products from hemicellulose contribute to the colour change of wood which becomes darker.

Nowadays, thermal modified wood has been extensively used and commercialized widely in Europe, for example, Thermowood in Finland, PlatoWood in Holland, Bois Perdure and Rectification in France (Esteves & Pereira, 2008; Rowell, 2005) and Termovuoto in Italy (Allegretti *et al.*, 2012). The main differences between the processes are found in the process conditions (process steps, oxygen or nitrogen, steaming, wet or dry process, use of oils, steering schedules etc.). The most widespread processes are carried out at atmospheric pressure and use gases (NO_2 or hot steam) as heating agents to eliminate oxygen and thus, prevent combustion of wood.

1.2.2 Wood protection by plant oil

Plant oil treated wood

Public concern about environmental issues urges industries to apply environmentally friendly technologies for wood protection. Thus, the

spotlight has fallen on impregnation of wood with renewable, non–hazardous and less expensive chemicals. As natural products, various plant oils have been applied for wood protection, particularly linseed, rapeseed, soybean, tall oil, palm and coconut oils. Except for coconut oil, most of the oils mentioned above are liquids at ambient temperatures. Plant oils have no fungicidal constituents but can inhibit wood decay fungi to some extent. Because the growth of fungi demands appropriate moisture, temperature, oxygen and nutrients to develop on wood, the effect of plant oils against fungi can be explained by 1) reduction in the wood MC and 2) decreased pore space due to the introduction of excessive oil and, thus the amount of oxygen required for fungal growth is substantially inhibited (Terziev & Panov, 2011). LO–treated Scots pine sapwood with low retention (156–208 kg m^{-3}) revealed no significant effect against the growth of the brown rot fungus *Coniophora puteana* as compared to untreated wood (Ulvcrona *et al.*, 2012). Tests according to the standard EN 113 (1996) indicated that LO retention for wood protection should exceed 320 kg m^{-3} to achieve an effective protection (Terziev & Panov, 2011; Sailer & Rapp, 2001). However, wood with high oil retention lead to problems, such as heavy weight and high cost, which is not industrially viable. Moreover, the scarcity of oxygen inside wood slow down the auto–oxidation of impregnated oil and, consequently, oils at high retention are prone to be exuded from wood. Improved durability can be achieved by simply mixing a small amount of fungicide (e.g. boric acid) with oil at low retention (Terziev & Panov, 2011), or synergic effect by mixing with pyrolysis bio–oil which itself contains antifungal phenolic compounds (Temiz *et al.*, 2013a). Wood extractives can also act as natural preservatives, showing effective resistance against wood decay fungi (Scheffer, 1966). Crude tall oil (CTO) is a major chemical by–product of pulp and paper industry which contains a complex mixture of wood extractives (Panov *et al.*, 2010; Koski, 2008; Biermann, 1993). CTO can be used as an effective wood protective agent for the protection of wood against decay fungi (Hyvönen *et al.*, 2007).

Meanwhile, the water repellence and dimensional stability of plant oil–treated wood have also been studied (van Eckeveld, 2001; van Eckeveld *et al.*, 2001b; van Eckeveld *et al.*, 2001a). Owing to the nature of hydrophobicity, plant oils can serve as water repellents which tend to reduce the rate of water absorption (Humar & Lesar, 2013; Ulvcrona *et al.*, 2012; Hyvönen *et al.*, 2006). The water repellents affect the wood by depositing on the pore surfaces or even filling in the cell lumens. As a consequence, water cannot be easily transported through the wood structure by capillary action, which reduces the rate of water uptake considerably (Dubey *et al.*, 2012). For drying oils, the auto–oxidation process can result in a tough and solid film by exposure to air,

serving as a protective layer on the wood surface. Microchecks and cracking in wood can be partly covered by impregnation with the plant oils (Jebrane *et al.*, 2015b; Humar & Lesar, 2013; Evans *et al.*, 2009). However, due to lack of covalent bonding between the water repellents and wood's hydroxyl groups, plant oils cannot fully prevent the process of water absorption. When wood is immersed in water for a long period of time, no significant difference in water uptake can be observed between wood treated with plant oils and untreated wood. Under normal circumstances, plant oils perform well for wood used in hazard class 2 (above ground covered) and class 3 (above ground uncovered) conditions due to their temporary inhibition of water absorption during rains (Humar & Lesar, 2013). In addition, since impregnated oils are not chemically bound with the cell wall, the effect of plant oil on the dimensional stability of wood is rather small (Dubey *et al.*, 2012).

Another drawback regarding oil–containing formulations for wood impregnation is the resulting high viscosity, which hinders the penetration and distribution of the solution in wood. The penetration of liquid is dependent on the size of molecule, MC, wood species and solvent. Studies showed that the maximum diameter of the cell wall micropores is about 2–4 nm (Hill, 2007). Molecules of impregnating agents greater than 0.68 nm in diameter may have difficulty in accessing to cell wall interior. Various techniques have been applied to assess the distribution of the impregnated agent in wood (Klüppel & Mai, 2013; Jensen *et al.*, 1992). The most common but time–consuming technique is to gradually take sub–samples from different depths of the specimen, and then measuring the chemical content or volume swelling of the sub–samples. Additionally, visual evaluation by scanning electron microscopy or fluorescent microscopy has been used to illustrate the penetration profile inside wood. Furthermore, X–ray densitometry has been implemented to monitor the permeability of impregnates inside wood (Olsson *et al.*, 2001). The ATR–FTIR (Attenuated total reflectance FTIR) was also regarded as an effective technique to measure penetration profile within wood, which use some characteristic peaks of the formulations components as internal standards to quantify the content of impregnated agent (Jensen *et al.*, 1992).

Epoxidized plant oil treated wood

As discussed above, the reactivity of plant oils can be improved by introduction of epoxy groups, which are realized by epoxidation of the double bonds at the fatty acid part of triglyceride. The ring opening reaction of epoxidized linseed oil requires either acidic or alkaline conditions (Saithai *et al.*, 2013; Panov *et al.*, 2010; Odian, 2004).

Jebrane *et al.* (2015a; 2015b) studied commercially available epoxidized linseed oil (ELO®)–treated wood samples by FTIR spectroscopy and confirmed the formation of new covalent carbon–oxygen bond between the epoxide groups and wood. The mechanism and viability of the ring opening reaction of ELO® by AA have been studied previously (Caillol *et al.*, 2012; Campanella *et al.*, 2010; Esteves & Pereira, 2008). Mixing epoxidized oil with AA can result in an increased viscosity owing to the formation of oligomers under acidic condition (Caillol *et al.*, 2012; Campanella *et al.*, 2010). ELO® in wood improves the dimensional stability (DS), water repellence and leaching resistance of Scots pine sapwood (Jebrane *et al.*, 2015a; Jebrane *et al.*, 2015b; Panov *et al.*, 2010). However, the excess use of AA is harmful and can pose potential corrosive problems to the equipment (reaction vessels, pipes, pumps, etc.). The reaction starts promptly after mixing AA with ELO®, but the viscosity of the mixture increases constantly with time even at ambient temperature, which can cause undesired clogging in the equipment. Although a two–step impregnation was suggested to overcome the short pot–life of the mixture, corrosion effect caused by AA cannot be avoided (Jebrane *et al.*, 2015a). The mechanical performances of ELO®–AA treated samples slightly decreases compared to untreated wood as a result of new materials introduced into the wood cell wall. Moreover, the impregnation of wood with AA separately contributed significantly to the loss of wood strength following the degradation of wood polysaccharides by AA (Jebrane *et al.*, 2015b). The mechanical properties of ELO® treated wood are comparable to bio–oil treated wood reported by Temiz *et al.* (2013b), which also demonstrated reduced mechanical properties of wood.

1.3   Wood modification by vinyl monomers

Graft copolymerization of vinyl monomers, such as methyl methacrylate and styrene, with wood components of the cell wall by gamma radiation or heating with catalyst was studied in the 1960s (Laidlaw *et al.*, 1967). Vinyl monomers can be introduced into the cell wall together with a wood swelling agent which facilitates the penetration of the monomers to the cell wall. Subsequent *in–situ* polymerization by gamma radiation is carried out forming graft copolymers, *i.e.* polyvinyl–polysaccharide copolymer. Using styrene or methyl methacrylate dissolved in methanol or dioxin as swelling agents, the effect of polymer loading on the dimensional stability of wood can be evaluated. Wood treated with PS or PMMA showed improved dimensional stability, but the PS–treated wood was reported to give higher anti–shrink efficiency than that of

PMMA–treated wood. The wood swelling agents used (either methanol or dioxan) showed little influence on wood anti–shrink efficiency.

1.4 Combination of VAc and plant oil as potential impregnating agent for wood modification

As a typical vinyl monomer, VAc is a colorless liquid which is mainly used as precursor to produce PVAc or the polyvinyl alcohol (PVA). As a low toxic and relatively cheap thermoplastic, PVAc found its application in the fields of wood and paper processing, civil engineering, packaging and binding industry adhesives and coatings, construction and civil engineering, textile and leather, biomedicine, etc. (Zhang *et al.*, 2013; Erbil, 2000). Waterborne dispersions containing PVAc have been extensively used as adhesives for wood or wood–based materials (Salvini *et al.*, 2010; Salvini *et al.*, 2009). However, the adhesive joints obtained with PVAc–based formulations suffer from poor moisture resistance, low heat and creep resistances (Zhang *et al.*, 2013; Petrie, 2007). Moreover, since PVA is generally used as protective colloid in emulsion polymerization of PVAc, the hydroxyl groups on the PVA lowers the water resistance of PVAc, which affects the performance of PVAc containing adhesive.

Modification of PVAc adhesive by additive modification, blending modification, copolymerization, protective colloid, modified initiator and emulsifier have been widely studied (Zhang *et al.*, 2013; Salvini *et al.*, 2009; Petrie, 2007). Drying oils can be used as co–monomers to copolymerize with VAc (Salvini *et al.*, 2010). The introduction of unsaturated triglycerides provides reactive sites for production of cross–linked adhesives with improved water resistance due to the incorporation of hydrophobic drying oils. However, the synthesis reported in the literature was performed by solution polymerization in organic medium, or in presence of hydrophilic protective colloid (Salvini *et al.*, 2010).

To integrate VAc and plant oil in water phase, small amounts of emulsifier(s) are needed to ensure a thermodynamically stable emulsion. Stable and homogenous emulsion without agitation facilitates wood impregnation in the stainless–steel impregnation reactor. Meanwhile, emulsions can be used to lower oil retention level, which can control the weight increase of treated wood after impregnation. The emulsifier, also known as surfactant, is usually composed of two parts, a hydrophilic head (polar) and a hydrophobic chain (nonpolar). When the concentration of surfactant reaches the critical micelle concentration (CMC), any additional surfactant added is aggregated to form micelles. The role of the emulsifier(s) is to help disperse monomers in the

water phase by reducing the interfacial tension between monomers and water. Depending on the electric charges on the head group of the emulsifier, the emulsifier can be categorized into four types, *i.e.*, anionic, cationic, amphoteric and non–ionic. The selection of appropriate emulsifiers takes into account a lot of factors. With respect to the emulsion polymerization of homopolymer PVAc, early studies selected anionic or anionic/non–ionic emulsifiers due to their great compatibility with negatively charged PVAc particles having persulfate initiator fragments (Erbil, 2000). However, no one to the best of our knowledge has studied the integration of vinyl ester with plant oils using efficient emulsifiers.

1.5   Objectives of the study

The overall objective of the work is to combine plant oil with VAc as impregnating agents for Scots pine (*Pinus sylvestris* L.) sapwood protection. In comparison to the only plant oil treated wood studied previously, the combination of VAc–plant oil formulation is aimed at avoiding the use of any acids as catalyst, since the acidic conditions can potentially cause corrosion to impregnation equipment. Moreover, the usage of acid initiates polymerization directly after mixing with ELO$^{®}$ even at room temperature, while the mixture of VAc–plant oil is stable at room temperature and copolymerization starts only upon heating. Oil exudation problems, typical for plant oil–treated wood is also expected to be solved by the formation of VAc–plant oil copolymer in wood. The present study has the following objectives:

➢ *Synthesis* and spectroscopic characterization of various degrees of epoxidized LO and SO.
➢ *Grafting* PVAc onto epoxidized oils with various epoxy content in the absence of organic solvent and protective colloid. Comparison between the obtained copolymers by means of gravimetric analysis, ATR–FTIR, ^{1}H–NMR and ^{13}C–NMR spectroscopy.
➢ *Optimization* of the process of impregnation with VAc–ELO$^{®}$ emulsion and subsequent curing. Study on the effects of solution uptake, curing temperature and time on the dimensional stability of the treated wood.
➢ *Characterization* of the VAc–ELO$^{®}$ treated wood by means of spectroscopy, microscopy, changes of physical–mechanical properties and durability.
➢ *Demonstration* of an additional application of ELO$^{®}$ combined with FA for wood protection.

2 Materials and methods

2.1 Materials

Table 1 lists the chemicals used in the entire study and their origin.

Table 1. *Chemicals used in the study.*

Name of Chemical	Supplier	Note
Brij® S 100	Sigma–Aldrich (Schnelldorf, Germany)	Polyoxyethylene stearyl ether, emulsifier, average M_n equals 4,670 g mol^{-1}
CTAB*	Sigma–Aldrich (Schnelldorf, Germany)	Cationic emulsifier
ELO®	Traditem GmbH (Hilden, Germany)	initial IV > 160, 0.1 residual double bonds per molecule
ESO®	Traditem GmbH (Hilden, Germany)	initial IV is not available
Furfuryl alcohol	Merck (Darmstadt, Germany)	$\geq$ 98%
Glacial acetic acid	Merck (Darmstadt, Germany)	100%
Hydrogen peroxide	VWR chemicals (France)	33%
LO	Oppboga Säteri, (Fellingsbro, Sweden)	–
Maleic anhydride	Kabo AB (Stockholm, Sweden)	$\geq$ 99%
Potassium persulfate	Merck (Darmstadt, Germany)	Initiator
SO	Traditem GmbH (Hilden, Germany)	–
Sodium carbonate	Sigma–Aldrich (Schnelldorf, Germany)	–
Sodium persulfate	Carl Roth GmbH (Karlsruhe, Germany)	Initiator
Span® 80	Sigma–Aldrich (Schnelldorf, Germany)	Sorbitane monooleate, non–ionic emulsifier
Sulfuric acid	Sigma–Aldrich (Schnelldorf, Germany)	95–98%
VAc	Sigma–Aldrich (Schnelldorf, Germany)	$\geq$ 99%, 3–20 ppm hydroquinone contained

*CTAB is the abbreviation of cetyltrimethylammonium bromide

The entire study was carried out on Scots pine (*Pinus sylvestris* L.) sapwood. Test samples were prepared according to standard EN 113 (1996) and ISO 3129 (1975) with dimensions of 20×20×340 mm (T×R×L) for mechanical tests and 15×25×50 mm (T×R×L) for swelling, leaching and durability tests. The samples were free from defects, splits, cracks, knots and the growth ring orientation of samples was as parallel as possible to the tangential longitudinal surface. By sawing the board along the grain, two matching samples were obtained, *i.e.* one was treated while the other served as control. Before impregnation, the samples were kiln dried and then conditioned at 20°C and 65% relative humidity (RH) until approximate 12% MC was achieved.

2.2 Instrumentation

ATR–FTIR spectra were acquired using a Perkin–Elmer FTIR spectrum one spectrometer on ATR mode with wavenumbers ranging from 4000 to 450 cm^{-1}. The sample to be analysed was brought into contact with diamond crystal of the ATR accessory and the spectra obtained were baseline–corrected and normalized. To investigate the effect of curing temperature and time on treated samples, samples after curing were split evenly along the grain to obtain two identical pieces. The mid–inner surface of the treated wood was brought into contact with diamond crystal, and spectra at different sites were recorded and averaged.

^{1}H–NMR and ^{13}C–NMR can be used in conjunction with ATR–FTIR to analyse the chemical structure of the synthesized polymers. NMR spectra were recorded at two laboratories by using Bruker Avance III 400 MHz and Bruker Avance III 600 MHz. Samples to be analysed were dissolved in CDCl$_3$ and chemical shifts were reported in δ (ppm) relative to residue solvent signal as the internal standard (CHCl$_3$, δ =7.26 ppm for ^{1}H–NMR and 77.23 ppm for ^{13}C–NMR).

Differential scanning calorimetry (DSC) was used as another thermo–analytical technique to determine the glass transition temperature (T_g) of polymers. Thermograms were obtained on a DSC Mettler–Toledo DSC 820 instrument under nitrogen atmosphere. A first heating ramp was necessary to erase the thermal history, and then the second heating ramp were carried out from −50°C to 200 °C at 10°C min^{-1}.

The micro–distribution of the treating agent inside wood samples was observed by light microscopy (Leica DMLB Wetzlar, Germany) and scanning electron microscopy (SEM, Philips XL30 ESEM operated at 10 kV).

Samples weight and dimensions were measured by a laboratory balance (Mettler, PM480 DeltaRange) with 0.001 g precision and a calliper (Mitutoyo digimatic indicator, Absolute 543–464B) with 0.01 mm precision, respectively.

The mechanical tests were performed using a universal testing machine (Shimadzu, AG–X 50 KN) with 0.01 mm precision for position, 0.1% for speed and 0.5% for loading.

2.3 Synthesis of partly epoxidized oils

SO or LO were mixed with glacial AA at room temperature. Then, H_2SO_4 (72%, w/w) was added dropwise into the solution under stirring at ambient temperature. As oxidizing agent, H_2O_2 (30%, w/w) was then added slowly to the solution by a funnel to avoid substantial increase of temperature due to the exothermic reaction between H_2O_2 and AA. It was reported that ring–opening reaction of the formed epoxy groups occurs at high temperature, which is detrimental for achieving high oxirane numbers (Campanella *et al.*, 2008). The present epoxidation experiment was carried out at moderate temperatures (30–50°C), by simply regulating the reaction time, a range of various degrees of epoxidized LO and epoxidized SO were obtained. The molar ratio of double bonds in oil: AA: H_2O_2 was kept at 1:1.5:0.5. The loading of H_2SO_4 was about 2% of the total weight of oil, H_2O_2 and glacial AA (Dinda *et al.*, 2008) (*Paper V*).

Table 2. *Reaction conditions for production of epoxidized LO and epoxidized SO with various epoxy.*

Oil	Molar ratio of reagents	Reaction condition
ELO1		30°C for 30 min, 40°C for 30 min, and 50°C for 7 h
ELO2		30°C for 30 min, 40°C for 30 min, and 50°C for 6 h
ELO3	Double bonds in oil:	30°C for 30 min, 40°C for 30 min, and 50°C for 3 h
ELO4	AA: H_2O_2 was	30°C for 30 min, 40°C for 30 min, and 50°C for 1 h
ESO1	1:1.5:0.5.	30°C for 30 min, 40°C for 30 min, and 50°C for 5 h
ESO2		30°C for 30 min, 40°C for 30 min, and 50°C for 3 h
ESO3		30°C for 30 min, 40°C for 30 min, and 50°C for 2 h
ESO4		30°C for 30 min, 40°C for 30 min, and 50°C for 1 h

Since the area under each signal in ^{1}H–NMR spectra is proportional to the amount of corresponding functional group, ^{1}H–NMR is used to quantify the epoxy content in different partly epoxidized oils. The signal of triglyceride at 4.12–4.31 ppm (–CH$_2$–CH–CH$_2$– of the glycerol moieties) was chosen as an

internal standard for quantification, which does not interfere with other signals and remains constant during epoxidation. The area under signal at 2.85–3.21 ppm (epoxy group, –C$\underline{H}$–O–C$\underline{H}$–) relative to the internal standard was used to calculate the number of epoxy groups in each oil molecule, from which the degree of epoxidation (DOE) can be calculated as follows (Saithai *et al.*, 2013; Farias *et al.*, 2010),

$$\text{DOE (\%)} = \frac{\text{number of epoxide groups}}{\text{number of starting double bonds}} \times 100\% \qquad (1)$$

We assumed that the ESO$^{®}$ and ELO$^{®}$ purchased directly from suppliers have higher DOE values than that of their corresponding synthesized partly epoxidized SO and partly epoxidized LO. However, since there was no available information regarding the number of starting double bonds, it was not possible to determine the exact DOE values for ESO$^{®}$ and ELO$^{®}$ in the present study.

2.4   Synthesis of homo– and copolymers

Small–scale synthesis of polyvinyl acetate (PVAc), VAc–plant oil copolymer s was carried out. The reagent VAc and oils were added to a water solution containing persulfate as initiator, and then transferred to a round–bottom flask equipped with stirrer and a reflux condenser. The influence of reagent amounts (ratio) and reaction conditions on the yields of copolymer are reported in Tables 8 and 9 (*Paper I*).

2.5   Emulsion preparation

To impregnate wood samples with the VAc–plant oil formulation, a stable and homogenous solution is required. Thus, emulsion was introduced to well integrate immiscible oil and water. Two ways of making homogenous emulsion were proposed here: 1) the screening test used emulsion of VAc–epoxidized LO with different epoxy content. It was prepared by dissolving water–soluble $K_2S_2O_8$ (0.25%, w/w) in deionized water, followed by addition of sodium carbonate (1%, w/w) and oil under constant agitation. Subsequently, non–ionic emulsifier Brij$^{®}$ S 100 (3%, w/w) and VAc were added. Although the yield of copolymerization increases with the increase of VAc content according to Table 8, by considering the low cost and eco–friendly nature of oil, the stoichiometric ratio of VAc, oil, and H_2O was kept at 1:1:1 by weight. 2) another way to prepare emulsion is to replace Brij$^{®}$ S 100 with the combined emulsifiers of CTAB (2.6%, w/w) and span$^{®}$ 80 (1.6%, w/w). Using combined CTAB and span$^{®}$ 80 avoid the impregnation problem of high viscosity solution

caused by the high molecular weight Brij® S 100. All emulsions were stirred in a beaker until a homogenous milky–coloured solution was obtained.

2.6 Characterization of treated samples

2.6.1 Determination of ASE and leaching rates

The wood samples were impregnated in a stainless–steel reactor. Rueping empty cell and full cell processes were employed to cover a wide range of solution uptake. The samples were moved to sealed glass containers after impregnation. Prior to the curing, a small amount of VAc monomers was poured at the bottom of container to create a saturated VAc condition to compensate the loss of impregnated VAc inside wood during the curing process. Subsequently, the samples were cured at various times and temperatures to study their effect on the weight percentage gain (WPG). Various impregnation schedules were also implemented at fixed curing time or temperature to investigate their impact on wood emulsion uptake and WPG. After curing all samples were dried at 103°C for 24 h. The WPG after drying is defined as:

$$\text{WPG (\%)} = \left[\frac{M_t - M_u}{M_u}\right] \times 100\% \quad (2)$$

where M_u and M_t are the oven–dry weight of samples before and after treatment respectively.

2.6.2 Swelling and leaching tests

Swelling test was carried out to study the dimensional stability of the treated samples by immersing them in deionized water for 48 h, followed by drying in an oven at 103°C for 24 h. Four cycles of water soaking and oven drying (WS–OD) were performed, and the dimension changes were recorded. The anti–swelling efficiency (ASE) was considered as a measure of the dimensional stability of wood in water, which is calculated as:

$$\text{ASE (\%)} = \left[\frac{S_u - S_t}{S_u}\right] \times 100\% \quad (3)$$

where S_t and S_u are the volumetric swelling coefficient of treated and untreated samples, respectively.

While the volumetric swelling coefficient S is defined as:

$$S\ (\%) = \left[\frac{V_w - V_d}{V_d}\right] \times 100\% \quad (4)$$

where V_w is the sample volume after humidity conditioning or water soaking, and V_d is the volume of oven–dried sample.

Simultaneously, a leaching test was accomplished by water according to the standard EN 84 (1997). The change in weight was measured before and after leaching to determine water leachability. Since the copolymer is soluble in acetone, treated samples after water leaching were subjected to the Soxhlet extraction with acetone for 7 h to remove all unbounded chemicals and then oven drying at 103°C for 24 h. The remaining copolymer after extraction was assumed to be chemically bound to the hydroxyl groups of the cell wall, while the copolymer in the cell lumen, rays, and resin canals was susceptible to dissolution and extraction by acetone. The presence of copolymer residues left in the wood after extraction can be verified by ATR–FTIR and the amount of copolymer left in wood after extraction can be determined gravimetrically, which can be expressed as:

$$P\,(\%) = \frac{WPG_a}{WPG} \times 100\% \quad (5)$$

where WPG is the initial WPG after curing and drying (before extraction), and WPG_a means the WPG after extraction. P is considered as the percentage of copolymer remaining in wood after extraction

2.6.3 Microscopy observations

Microscopy observations were carried out by means of both light microscopy and SEM. Samples for light microscopy were cut from the centre of treated wood and soaked in deionized water for overnight. Transverse, radial longitudinal, and tangential longitudinal sections (approx. 50 μm) of treated wood were cut using a sliding microtome. Since the impregnated copolymer in treated wood can be stained by oil–soluble Sudan III stain which is suitable for colouring nonpolar substances such as fats, waxes, and triglycerides (Patel *et al.*, 2015), the staining process was performed by immersing sections in a saturated solution of Sudan III in 70% ethanol (w/v) for 5 min. Finally, coverslips were mounted over the sections using 50% (v/v) glycerol in deionized water.

For SEM, sections (approx. 50 μm) of treated samples were dried overnight at 30°C, and then mounted on stubs with double–sided tape and coated with an approximately 6 nm layer of gold using a sputter coater. Sections were observed using a Philips SEM.

2.6.4 Mechanical properties

The treatment of wood with VAc–ELO® resulted in significant decrease in water adsorption. Since changes of EMC in the cell wall have impact on the mechanical properties, treated and untreated wood samples were conditioned separately at different climate conditions to achieve the same level of EMC.

Wood sampling methods and general requirements for mechanical tests were prepared in accordance to ISO 3129 (1975). The mechanical properties measured included:

➢ Modulus of elasticity (MOE) according to ISO 3349 (1975).
➢ Modulus of rupture (MOR) according to ISO 3133 (1975).
➢ Brinell hardness parallel (‖) and perpendicular (⊥) to the grain according to ISO 3350 (1975).
➢ Compression stress parallel (‖) and perpendicular (⊥) to the grain according to ISO 3787 (1976) and ISO 3132 (1975) respectively.
➢ Shear strength parallel (‖) to the grain according to ISO 3347 (1976).
➢ Impact bending strength according to ISO 3348 (1975).

2.6.5 Durability testing of the modified wood

Screening test was performed on wood treated with VAc–epoxidized LO having different epoxy content for the evaluation of decay resistance. Samples measuring $5\times15\times40$ mm were leached according to the standard EN 84 (1997) and after re–conditioning they were exposed to the white rot fungus (*Trametes versicolor*) and the brown rot fungi (*Gloeophyllum trabeum, Postia placenta*, and *Coniophora puteana*) in a climate room (25°C and 65% RH). After 9 weeks' incubation, the samples were cleaned gently and the wet weights were measured. After drying at 103°C for 24 h, resistance against fungi was evaluated by measuring the mass loss (ML). Later, standardized tests (EN 113) were performed using samples with dimension of $15\times25\times50$ mm to test the durability of VAc–ELO® treated wood at different WPG. After leaching according EN 84 (1997) and re–conditioning, samples were exposed to the white rot fungus (*Trametes versicolor*) and brown rot fungi (*Lentinus lepideus, Postia placenta*, and *Coniophora puteana*) for 16 weeks' in the same condition as the screening test. Classification of durability class (DC) was carried out according to the standard EN 350–1 (1994). ML of the treated wood was compared with the ML of untreated wood and classified in five DCs as follows: 1–very durable, 2–durable, 3–moderately durable, 4–slightly durable, and 5–non–durable (*Paper III*).

The ML described in the thesis refers to the corrected ML, in which the ML of correction samples is taken into account. The ML of correction samples correspond to the average ML of treated samples in the test without fungal attack. The corrected ML is defined as,

$$\text{Corrected ML(\%)} = \text{ML} - \text{ML of correction samples} \qquad (6)$$

3   Results and discussion

3.1   Synthesis and characterization of oils derivatives and copolymers

3.1.1 Spectroscopic characterization of oils with various epoxy content

The ^{1}H–NMR spectra of LO, ELO® and four synthesized partly epoxidized LO are revealed in Figure 3.
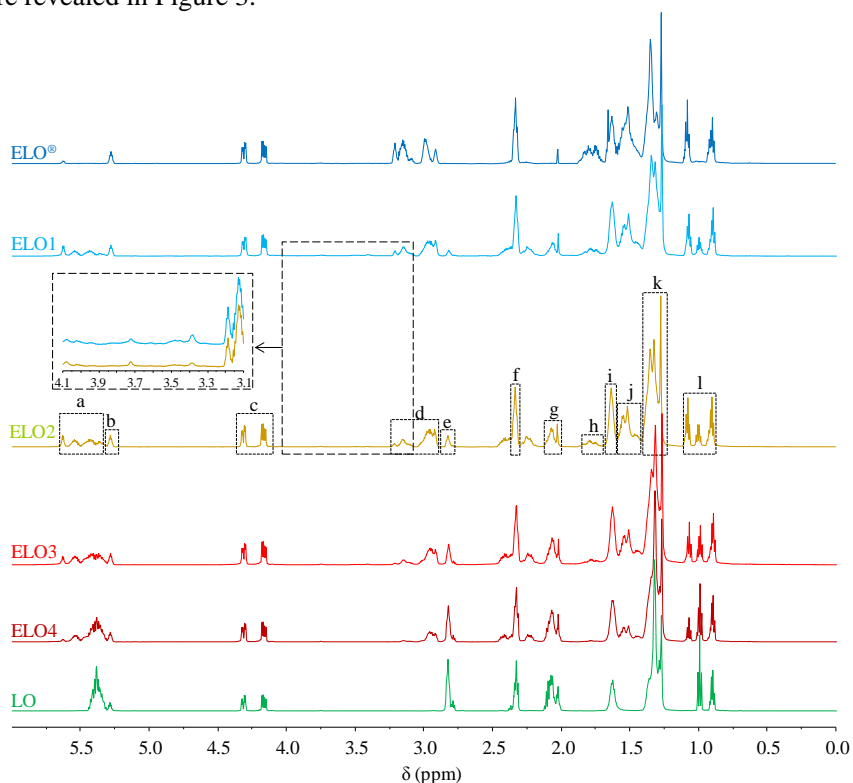
Figure 3. ^{1}H–NMR spectra of LO, ELO® and partly epoxidized LO (*i.e.* ELO1, ELO2, ELO3, ELO4, in which ELO1 has the highest epoxy content while ELO4 has the lowest epoxy content). Signal at 3.3–4.1 ppm for ELO1 and ELO2 are enlarged.
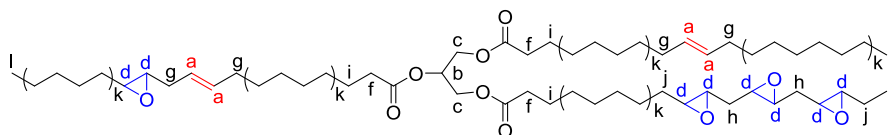
Figure 4. Chemical structure of partly epoxidized oil. The letters for each proton coincide with those shown in Figure 3.

Since similar ^{1}H–NMR spectra can be observed for SO and its derivatives apart from the intensity difference in the regions of double bonds and epoxy groups, only the spectra of LO and its derivatives are shown here (*Paper I* and *V*).

Table 3. *Assignment of signals in ^{1}H–NMR spectra for partly epoxidized LO. The letters in Table are in line with those shown in Figure 3.*

Signal	Chemical shift δ (ppm)	Structure with assignment
a	5.29–5.68	–CH=CH–
b	5.23–5.28	–CH₂–CH–CH₂– of the glycerol backbone
c	4.12–4.31	–CH₂–CH–CH₂– of the glycerol backbone
d	2.85–3.21	>CH– at epoxy group
e	2.75–2.82	–CH=CH–CH₂–CH=CH–
f	2.27–2.35	α–CH₂ to the carbonyl group –OCO–CH₂–
g	1.97–2.11	–CH₂–CH=CH– in acyl chain
h	1.68–1.85	α–CH₂– adjacent to two epoxy groups
i	1.56–1.67	β–CH₂ to the carbonyl group –OCO–CH₂–CH₂–
j	1.39–1.56	α –CH₂– to epoxy group
k	1.20–1.39	saturated methylene group –(CH₂)ₙ– in acyl chain
l	0.84–1.09	terminal –CH₃
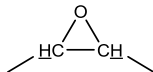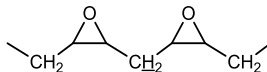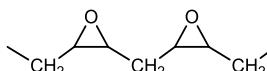
The process of oil epoxidation converts double bonds in triglyceride molecules to epoxy groups. However, residual double bonds still remain after reaction due to incomplete epoxidation. The chemical structure of a typical partly epoxidized oil is illustrated in Figure 4. Assignments for signals based on the partly epoxidized LO in the range of δ = 0–6 ppm are displayed in Table 3 (Xia *et al.*, 2015; Saithai *et al.*, 2013; Oyman *et al.*, 2005; Adhvaryu & Erhan, 2002). The characteristic signals of ELO® can be observed at 2.85–3.21 ppm for epoxy groups and at 1.39–1.56 ppm and 1.68–1.85 ppm for α–CH₂– to epoxy groups. An enlargement of this region allows distinguishing between

mono–epoxides at 2.85–3.03 ppm, and adjacent epoxides at 3.04–3.21 ppm. Signals for the double bonds in LO are observed at 5.29–5.47 ppm, and the signals for the α–C$\underline{H}_2$ to the double bonds in LO are shown at 1.97–2.11 ppm and 2.75–2.82 ppm. Regarding partly epoxidized oil, signals attributable to the double bond adjacent to epoxy group are observed at 5.48–5.68 ppm.

As the area under each ^{1}H–NMR signal is proportional to the quantities of equivalent protons in the molecule, the "number of epoxy groups" per each oil molecule can be determined by measuring the area of the signal at *d* (δ=2.85–3.21 ppm). By assuming the area of internal standard at *c* (δ=4.12–4.31 ppm) to be 4, the area under signal at *d* is obtained (Table 4), and the value of DOE is also determined according to Equation (1). Since all the partly epoxidized LO or epoxidized SO were synthesized from LO or SO, the number of double bonds present in LO or SO can be regarded as the "number of starting double bonds" in Equation (1), which can be obtained by measuring the area of the signal at *a* (δ=5.29–5.68 ppm) in LO or SO. However, for the ELO[®] and ESO[®], since they were purchased directly from suppliers and used as received, the epoxidation methods and origin of their corresponding LO and SO are unknown. Consequently, the DOE of ELO[®] and ESO[®] cannot be determined in this study. As shown in Table 4, increasing the time of the epoxidation reaction results in an increase of DOE. By comparison, Farias *et al.* (2010) studied the epoxidation of SO at 110°C using bis(acetyl–acetonato)dioxo–molybdenum as catalyst in the presence of *tert*–butyl hydroperoxide as oxidizing agent. The 2–24 h reaction resulted in DOE in the range of 41–54%, which is comparable to the epoxidation method described in the present study.

According to Table 2, there is a one hour heating difference between the reaction condition to obtain ELO1 and ELO2, however, the difference in DOE between ELO1 (56.5%) and ELO2 (55.8%) is small. It can be explained by the side reaction of the acid–catalyzed ring opening of the epoxy groups due to the presence of H_2SO_4 and AA in the solution. Epoxidation carried out at high temperatures or long time contributes to the loss of epoxy groups. It was reported that protons in α position of secondary hydroxyl caused by ring opening of epoxide (C$\underline{H}$–OH) and protons in α position of ether link due to oligomerization (C$\underline{H}$–O–CH) show signals at 3.3–4.1 ppm (Caillol *et al.,* 2012). The intensity difference between ELO1 and ELO2 in the region of 3.3–4.1 ppm is highlighted in Figure 3. Compared to the ELO2, the ELO1 shows higher signal intensity at 3.3–4.1 ppm which is presumably caused by the acid–catalyzed ring opening of the epoxy groups. Consequently, the DOE of ELO1 is close to that of ELO2 in spite of difference in epoxidation time.

Table 4. *Measured area under signal at* **d** *(δ=2.85–3.21 ppm) of partly epoxidized oils for determination of DOE (%).*

	Area under signal at d (δ=2.85–3.21 ppm)	DOE (%)
Linseed oil		
ELO®	11.00	–
ELO1	6.99	56.5
ELO2	6.90	55.8
ELO3	5.65	45.7
ELO4	3.31	26.8
LO*	0	–
Soybean oil		
ESO®	7.96	–
ESO1	5.53	69.0
ESO2	3.95	49.3
ESO3	3.15	39.3
ESO4	2.32	28.9
SO*	0	–

* The area under signal a (δ=5.29–5.68 ppm) in the spectra of LO and SO was 12.36 and 8.01 respectively.

Table 5 shows the peak assignment of LO and ELO® at wavenumbers 4000–450 cm^{-1}. The characteristic absorption peak of epoxy group is found at 821 cm^{-1}, which is not present in the LO spectrum. Nevertheless, the LO spectrum is characterized by double bond absorption at 3011 and 1654 cm^{-1}, which is not seen in the ELO® spectrum. The characteristic peaks of both epoxy groups and double bonds appear in the spectrum of partly epoxidized LO, but their intensities are comparatively weaker.

Table 5. *Assignment of characteristic peaks in ATR–FTIR spectra for ELO® and LO.*

Wavenumbers (cm^{-1})	Peak assignment
Peak shown in both ELO® and LO	
2962, 2925, 2855	ν_{as}(C–H)CH$_3$, ν_{as}(C–H)CH$_2$, ν_s(C–H)CH$_2$
1740	ν(C=O) in ester
1458	δ_a(CH$_2$)
1388	δ(CH$_2$)
1243, 1157, 1098, 1019	ν(C–O) and ν_a(C–O) in ester
726	ρ(CH$_2$)n and ω(C–H)=CH
Characteristic peak for either ELO® or LO	
3011	ν(C–H)=CH
1654	ν(C=C)
821	ν(C–O–C, epoxide)

The ATR–FTIR spectra of initial LO, partly epoxidized LO (using ELO2 as representative) and ELO® are compared in Figure 5. The peak corresponding to the stretching vibration of epoxy group at 821 cm^{-1} has been magnified in Figure 5 to calculate the change of peak area upon epoxidation.
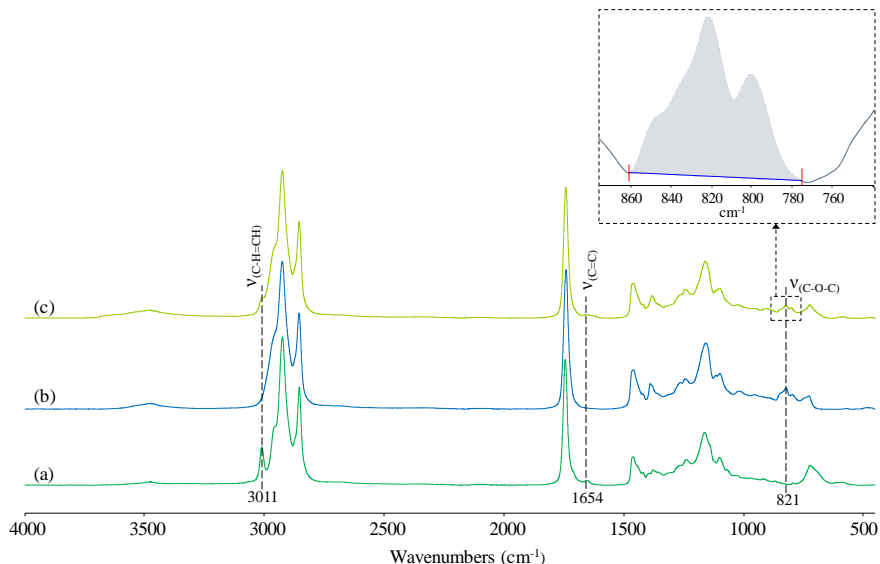

Figure 5. ATR–FTIR spectra of LO (a), ELO® (b) and partly epoxidized LO (c) together with enlarged scale of peak (epoxy group) at 821 cm^{-1}

Investigation of the ATR–FTIR spectra of SO, partly epoxidized SO and ESO® are comparable to the spectra shown above, therefore, the comparison among SO, partly epoxidized SO and ESO® are not shown here.

Table 6. *Area under FTIR peak at 821 cm^{-1} for epoxidized LO and epoxidized SO at various degree of epoxidation.*

Oil type	ELO®	ELO1	ELO2	ELO3	ELO4	LO
Area	1.99	1.09	1.08	0.74	0.34	0
Oil type	ESO®	ESO1	ESO2	ESO3	ESO4	SO
Area	0.86	0.57	0.36	0.28	0.22	0

According to Beer–Lambert law, the absorbance is proportional to the concentration of the analyte. The peak area at 821 cm^{-1} is thus proportional to the number of epoxy groups in oil, which can be used to estimate the epoxy content. Since the area under signal of ^{1}H–NMR spectra at δ=2.85–3.21 ppm

can be used to determine the number of epoxy groups in oil, the correlation between ATR–FTIR and ^{1}H–NMR in measuring the epoxy content in oil molecule can be obtained, as shown in Figure 6. The area of ATR–FTIR spectral peak is measured at 821 cm^{-1} while ^{1}H–NMR spectral area takes into account the area under signal at δ=2.85–3.21 ppm. The peak area ratio (partly epoxidized LO/ELO® and partly epoxidized SO/ESO®) obtained from ATR–FTIR spectra is plotted as function of signal area ratio calculated from ^{1}H–NMR. As seen in Figure 6, the area ratio obtained from ATR–FTIR increases with the increase of the area ratio determined from ^{1}H–NMR with linear regression coefficients of 0.96 for partly epoxidized LO and 0.99 for partly epoxidized SO respectively, indicating strong correlation between the two characterization methods for determination of the epoxy content.
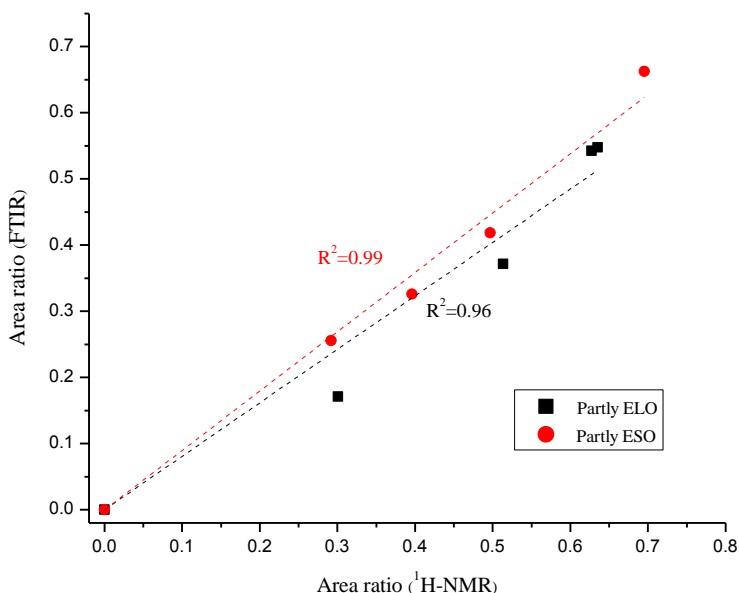

Figure 6. Fitted linear relationship between the peak (signal) area ratio measured by ATR–FTIR and ^{1}H–NMR regarding the epoxy content in oil molecule.

3.1.2 Synthesis of copolymers and their spectroscopic characterization

In order to investigate the reactivity of epoxidized oils with various epoxy content on the production of VAc–oil copolymer, gravimetric analysis was performed on products by reacting VAc with various degrees of epoxidized LO or epoxidized SO in presence of radical initiator (Table 7). The feed ratio of VAc to oil was kept at 1:1 (w/w) and the synthesized copolymer was first washed with deionized water, followed by diethyl ether to remove the residual unreacted oil.

Table 7. *The yield of copolymer by reacting VAc with various degrees of epoxidized LO or epoxidized SO (VAc/oil=1/1, w/w) at 80°C for 2 h with 0.25% initiator.*

	DOE (%)	Yield (%) after reaction with VAc
Linseed oil		
ELO®	–	54.3
ELO1	56.5	49.2
ELO2	55.8	37.6
ELO3	45.7	1.3
ELO4	26.8	oligomers
LO	–	oligomers
Soybean oil		
ESO®	–	53.8
ESO1	69.0	47.5
ESO2	49.3	46.3
ESO3	39.3	47.6
ESO4	28.9	49.4
SO	–	50.6

For the reaction between VAc and epoxidized LO with various epoxy content, the reaction involving epoxidized LO with high epoxy content tend to yield more polymer than the epoxidized LO having relatively low epoxy content (Table 7). The reaction between VAc and LO or even epoxidized LO with lower epoxy content (e.g. ELO3, ELO4) does not produce polymers after 2 h reaction. Regarding SO and its derivatives, the signals corresponding to the oil moieties can hardly be identified in products obtained after reaction between VAc and SO or its derivatives according to the spectroscopic analysis. Their resulting spectra are analogous to that of the homopolymer PVAc. Figure 7 compares the spectra among products after reaction between VAc–ESO, VAc–ELO3, VAc–ELO2, VAc–ELO1 and VAc–ELO® in the range of 2.9–5.5 ppm. Signals attributable to oil fragments can only be found in the spectra of VAc–ELO®, VAc–ELO1 and VAc–ELO2 in which the epoxidized oils used have high epoxy content. By contrast, spectra of VAc–ESO and VAc–ELO3 show only PVAc signals. Based on the results shown above, it is assumed that epoxidation of the double bonds in oil activates the residual double bonds in oil, which could be explained by the change of inductive effect due to the epoxidation of some double bonds. The reaction between VAc and epoxidized oil depends not only on the degree of epoxidation in oil but also on the types of oil used (*i.e.* epoxy content). Consequently, maximum epoxidized LO is considered as the most reactive monomer compared to the other partly epoxidized LO and epoxidized SO in copolymerization reaction with VAc.
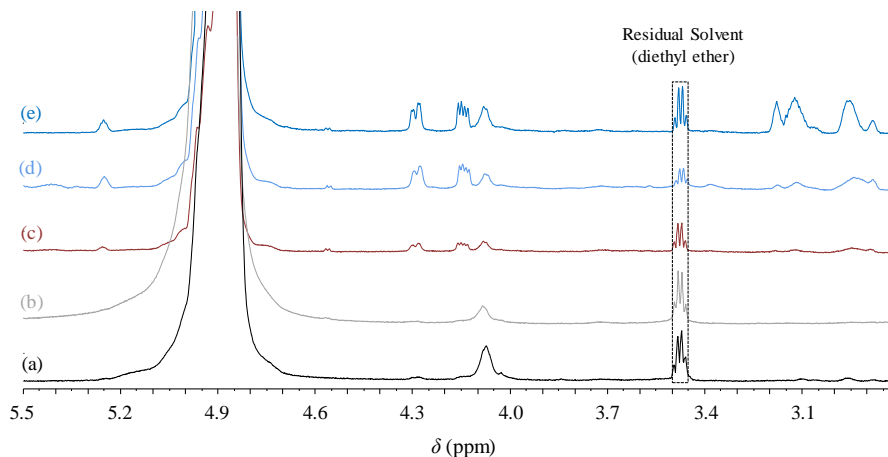
Figure 7. ^{1}H–NMR spectra of VAc–ESO® (a), VAc–ELO3 (b), VAc–ELO2 (c), VAc–ELO1 (d), VAc–ELO® (e) copolymer/polymer, the ratio of VAc/oil=1/1 (w/w).

As the most reactive monomer in our study, ELO® has been further studied and subjected to reaction with VAc in varied conditions to evaluate their effect on the conversion of monomers to copolymer. As shown in Table 8, a negative effect of high ELO® amount on the copolymer's yield is observed, which can be explained by the relatively low reactivity of the free triglycerides caused by steric hindrance and polyunsaturated fatty chain in ELO. Experiments on the reactivity of ELO® with radical initiator were also investigated previously by ^{1}H–NMR and no structural difference can be observed for ELO® before and after reaction. Therefore, the yield of only ELO® monomer reacting with radical initiator is assumed to be 0% (*Paper I*). Similar results were obtained for the reaction between LO and VAc in organic solvent (ethyl acetate), where the yield decreased from 69.4% to 44.2% when the feed ratio of LO/VAc increased from 10% to 30% (Salvini *et al.*, 2010).

Table 8. *Effect of feed ratio of VAc/ELO® on the copolymer yield at 80°C for 2 h with 0.25% initiator.*

Feed ratio	Only VAc	VAc–ELO® copolymer			Only ELO®
		VAc/ELO®=3/1	VAc/ELO®=1/1	VAc/ELO®=1/3	
Yield (%)	93.7	91.3	54.3	24.4	0

Table 9. *Effect of reaction conditions (time, temperature and catalyst amount) on the yield of VAc–ELO® copolymer (VAc/oil=3/1, w/w).*

Reaction time (min)	30	60	120	240	360
Yield (%)*	4.2	74.2	91.3	89.2	94.6
Reaction temperature (°C)	60	70	80	90	100
Yield (%)**	0.6	85.2	91.3	91.2	93.3
Catalyst amount (%)	0.05	0.1	0.25	0.5	1
Yield (%)***	13.0	80.7	91.3	90.4	91.0

* Reaction temperature was 80°C and initiator amount was 0.25%.
** Reaction time was 2 h and initiator amount was 0.25%.
*** Reaction time was 2 h and reaction temperature was 80°C.

As shown in Table 9, the yield of reaction is found to increase with increasing reaction time, temperature or catalyst amount. It is probable that the yield of copolymer (VAc/oil=3/1, w/w) reaches a plateau after 120 min at 80°C with 0.25% initiator, providing yield of more than 90%. Apart from the experiments mentioned above, no reaction occurs in the absence of initiator or water, which proves the importance of catalyst and water in the process of copolymerization.
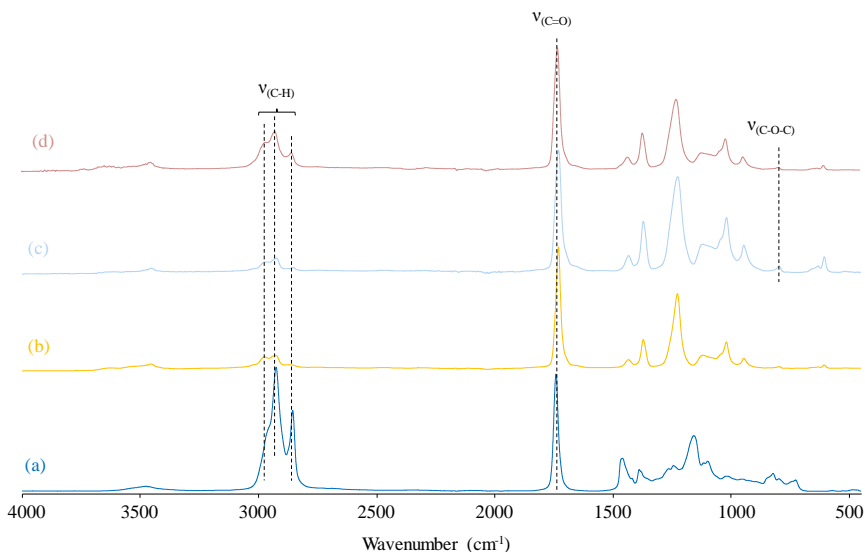

Figure 8. ATR–FTIR spectra of ELO® (a), PVAc (b), VAc–ELO2 copolymer (c), and VAc–ELO® copolymer (d) (VAc/oil=1/1, w/w).

According to the Table 8, the feed ratio VAc/ELO®=3/1 resulted in the highest yield (91.3%) compared to the feed ratio of 1/1 (54.3%) and 1/3 (24.4%). However, by considering the low cost and eco–friendly nature of ELO®, the

1/1 feed ratio was chosen to reduce VAc content in the formulation for the following characterization. ATR–FTIR was applied to prove the reaction between VAc and ELO® or ELO2 by identification of the characteristic peaks from both reagents. In Figure 8, a shift in the characteristic absorption peak of the epoxy group (821 cm^{-1}) to lower wavenumbers (798 cm^{-1}) with decreased intensity is observed in the copolymer. The spectrum of synthesized copolymer shows three distinct absorption peaks in the range 2850–3000 cm^{-1}, which are attributed to C–H stretching vibration originating from ELO® and PVAc. Compared to the spectrum of PVAc, the absorption peaks shown in the range of 2850–3000 cm^{-1} in ELO® are stronger than PVAc. The spectrum of VAc–ELO® copolymer shows higher peak intensities at 2850–3000 cm^{-1} than VAc–ELO2, which implies more oil in VAc–ELO® copolymer and indicates a higher reactivity of VAc towards ELO® than ELO2.
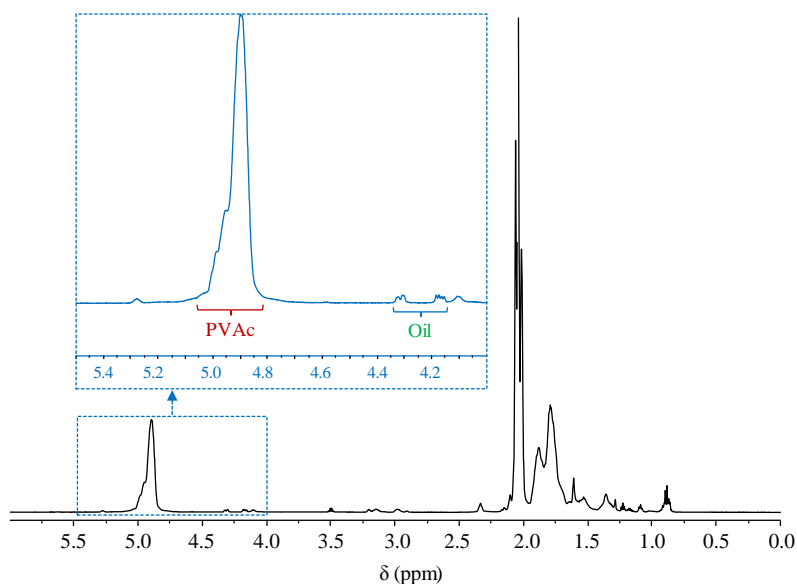
Figure 9. ^{1}H–NMR spectrum of VAc–ELO® copolymer (VAc/oil=1/1, w/w).

Figure 9 shows the spectrum of VAc–ELO® copolymer after reaction at 80°C for 120 min with 0.25% catalyst. Similar spectra can be obtained by reacting VAc with epoxidized LO having high epoxy content. According to the spectrum, the signals from both ELO® and PVAc are visible, which suggests the coexistence of the two compounds. The signals at 1.77, 2.02 and 4.87 ppm in the spectrum are attributable to the PAVc backbone, while signals attributable to the ELO® fragments can be seen at 5.61 (–C<u>H</u>=C<u>H</u>–), 5.25, 4.12–4.31, 2.85–3.21 (epoxy groups), 2.31, and 0.84–1.09 ppm. However, due

to the low reactivity and higher molecular weight of the triglycerides, the intensity of the signals attributable to ELO[®] fragment appeared to be small compared to that of the signals corresponding to the PVAc shown in the spectrum.

The required amount of oil with regard to the amount of VAc in the synthesized copolymer can be estimated by ^{1}H–NMR. The area under signal at 4.12–4.31 ppm (–CH$_2$–CH–CH$_2$– of the glycerol backbone in triglyceride) and 4.78–5.07 ppm (PVAc methine) are used to represent the oil and PVAc fragments respectively for quantification. The area under signal of double bonds in ELO[®] decrease significantly in presence of PVAc, which implies the reaction between PVAc and ELO[®] through the residual double bonds in ELO[®]. The molar ratio of oil/VAc in the copolymer was calculated as 0.87, 0.85 and 0.74 mol.% for VAc–ELO[®], VAc–ELO1, VAc–ELO2 formulations respectively.
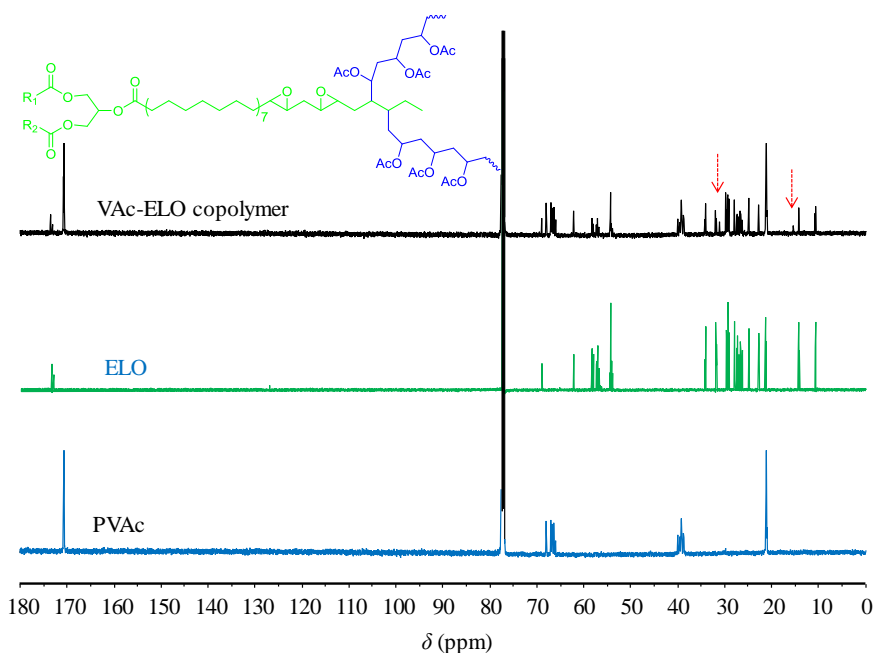
Figure 10. ^{13}C NMR spectra of PVAc, ELO[®] and VAc–ELO[®] (VAc/ELO[®] =1:1 by weight) copolymer with structure showing the PVAc grafting to the ELO[®] molecule.

The grafting of PVAc to the triglyceride has been proven by ^{13}C–NMR. As seen in Figure 10, signals at 173.2–173.3 and 170.4 ppm attributable to the ester carbonyls in triglyceride and PVAc respectively appear in the ^{13}C–NMR spectrum of VAc–ELO[®] copolymer. However, the signal at 126.8 ppm

(CH=CH in oil) disappear in the copolymer spectra, which indicates the participation of double bonds in the copolymerization with VAc. Meanwhile, two new signals are observed at 31.0 and 15.3 ppm in the copolymer spectrum, which correspond to the carbons of ELO®–CH–CH–PVAc linkage. Therefore, the reaction route for the synthesis of VAc–ELO® copolymer can be assumed in two steps. The first step involves a radical initiation of VAc polymerization in presence of persulfate. During the second step, the propagation of VAc monomers takes place, and the formed radical intermediate reacts with residual double bonds in triglyceride molecule. A grafted polymer can be obtained after the termination step (disproportionation or combination of radical intermediates).

3.1.3 Thermal analysis

As one of the principal characteristic related to polymer properties and processing, the T_g of ELO®, poly-ELO® (PELO®), PVAc, VAc–ELO® copolymer and PVAc/PELO® blend were determined by means of DSC. For amorphous or semi–crystalline polymers, a blend of two incompatible polymers generally shows two distinct T_g, while a random copolymer obtained from reaction of two monomers exhibits one T_g which appears between the two T_g of the corresponding homopolymers.
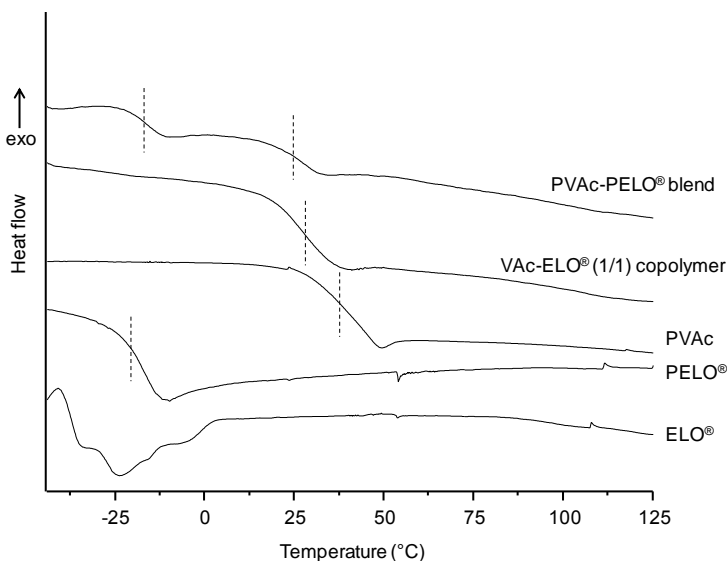

Figure 11. DSC thermograms of ELO®, PELO®, PVAc, VAc–ELO® copolymer (VAc/oil=1/1, w/w) and PVAc/PELO® blend**.**

As shown in Figure 11, the formation of VAc–ELO® copolymer (VAc/oil=1/1, w/w) was proved by the presence of a single T_g at approximately 25°C upon heating, which is lower than that of PVAc homopolymer (38°C) due to the plasticizing effect caused by the introduction of more flexible ELO®. Regarding the monomer, ELO® shows peaks of crystallization before melting caused by the different crystalline polymorphs (Guo *et al.*, 2000).

3.2   Wood impregnation

3.2.1 Effect of curing temperature and time

The spectra of treated samples obtained after curing are normalized according to the peak at 1509 cm^{-1} (Figure 12). The area under the peaks at 1650 cm^{-1} and 1509 cm^{-1} are used to monitor the extent of curing inside wood. The areas under the peaks are determined based on the baseline method which is constructed by extrapolating a line between the valleys at 1683–1538 cm^{-1}, and 1538–1487 cm^{-1}, respectively (*Paper II*). As an internal standard, the peak at 1509 cm^{-1} is attributable to the aromatic skeletal vibration of lignin (Glasser & Jain, 1993; Schultz & Glasser, 1986), which is not involved in the reaction. The peak at 1650 cm^{-1} corresponds to the C=C stretching in the unreacted VAc monomer. Since VAc and ELO® monomers are consumed during curing process, the amount of VAc remained relative to the internal standard can be used to estimate the progress of curing.
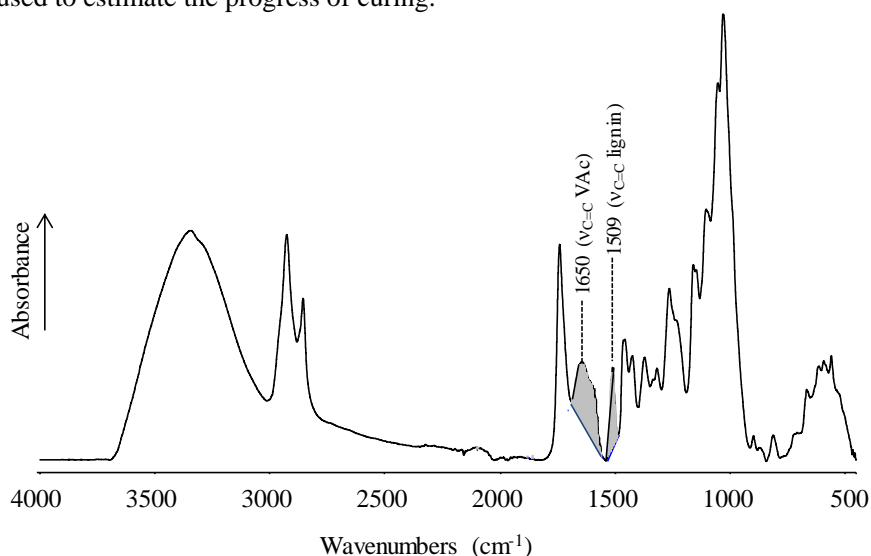

Figure 12. FTIR spectrum of VAc–ELO® (VA/ELO®=1:1, w/w) treated wood after curing showing the main characteristic peaks at 1650 cm^{-1} and 1509 cm^{-1} which are used to monitor the curing process.

The extent of curing at predetermined temperatures is evaluated by calculating the peak area ratios of A_{1650}/A_{1509} in each spectrum and plotted against curing temperature, as shown in Figure 13. A linear relationship between peak area ratio and temperature is obtained with high regression coefficients (R^2=0.91). Since the aromatic band at 1509 cm^{-1} is not involved in the reaction, the decreasing ratio A_{1650}/A_{1509} with increasing temperature is mainly due to the change of area under the peak at 1650 cm^{-1}. The peak area at 1650 cm^{-1}, which results solely from C=C of VAc, decreases as the VAc reacts with either another VAc monomer or ELO$^®$ through radical polymerization. Additionally, the influence of curing temperature on WPG after treatment and the ASE of wood after one cycle of WS–OD is also shown in Figure 13. The WPG obtained at the studied curing temperatures are not statistically different, ranging from 20.7% to 23.7%, which is in agreement with previous findings in which the yield of copolymer reaches a plateau at 80°C. However, the ASE of VAc–ELO$^®$ treated wood increases with temperature. The improved dimensional stability at high curing temperature is attributed to the long-chain polymer built at high temperature. Nevertheless, from energy saving and economical point of view, curing at 90°C seems to be adequate to improve the dimensional stability of wood (ASE=31.2%), although higher temperatures can provide higher ASE.
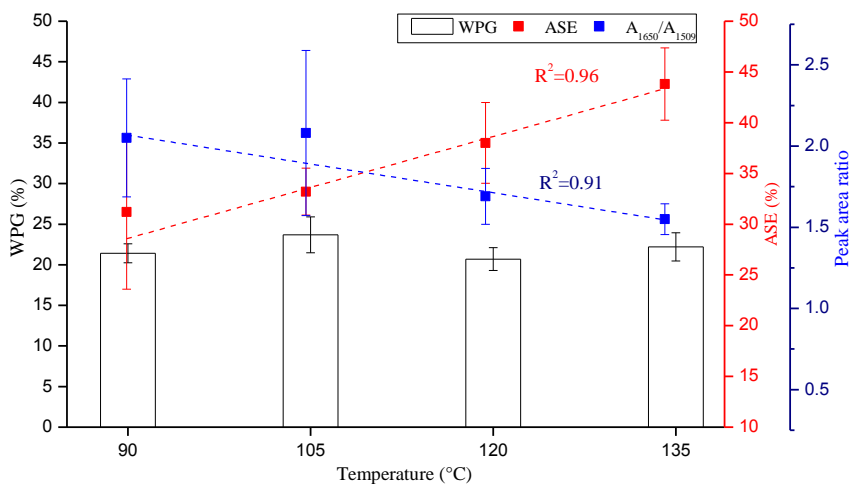

Figure 13. The WPG (%), ASE (%) and peak area ratio (A_{1650}/A_{1509}) of wood treated with VAc–ELO$^®$ (1/1, w/w) at different temperatures for 96 h.

The impact of curing time on the WPG, ASE and peak area ratio is illustrated in Figure 14. The increased curing time results in a decreased peak area ratio A_{1650}/A_{1509}, which is comparable to the effect of increasing temperature

described in Figure 13. The WPG after treatment and the dimensional stability (ASE) of wood are also plotted as function of curing time in the Figure. There is no significant difference in WPG (19.6–23.6%) as the curing time increases, which is also in line with our previous finding in yield showing negligible effect of curing time on the WPG after 2 h. By contrast, long time curing in the oven produces wood with improved dimensional stability, and a linear relationship (R^2=0.98) is assumed between the ASE and curing time. However, from energy saving and economical point of view, curing at 90°C for 168 h appears to be adequate to achieve a satisfactory dimensional stability.
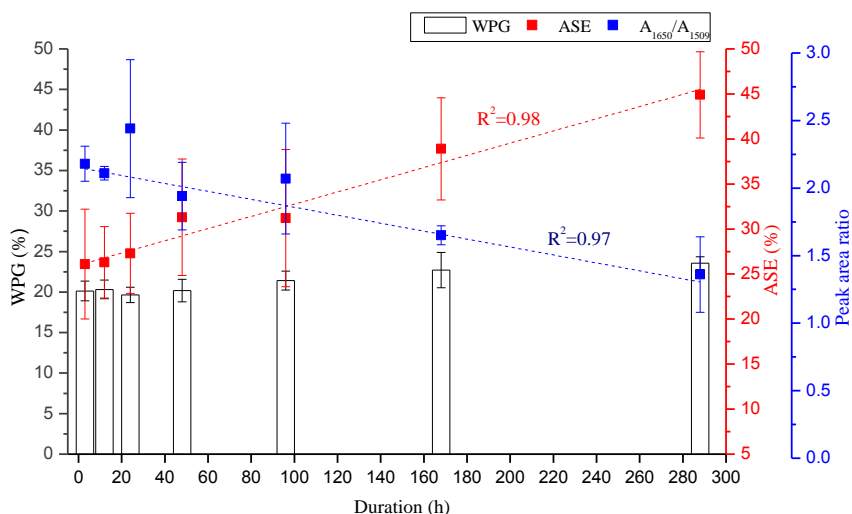
Figure 14. The WPG (%), ASE (%) and peak area ratio (A_{1650}/A_{1509}) of wood treated with VAc–ELO® (1/1, w/w) for different durations at 90°C.

3.2.2 Correlation between WPG and ASE

In order to investigate the impact of WPG on ASE, four impregnation schedules were designed to study the influence of solution uptake (VA/ELO®=1:1, w/w) on wood dimensional stability after cycles of WS–OD. Samples after different impregnation schedules were cured at 90°C for 168 h. According to Table 10, it can be assumed that the VAc–ELO® treated wood can produce dimensionally stable wood, but the increased uptake cannot improve ASE to a great extent. Wood samples of 8.6% WPG ensures an ASE of 37.7–39.5% while 37.1% WPG leads to ASE of 43.6–46.5%. Previous studies reported wood samples treated with a mixture of ELO® and AA (12.0–46.2% WPG) resulted in significant DS improvements (39.8–56.6% ASE), but the retention had only a small or even negligible correlation with ASE (Jebrane *et al.*, 2015a), which coincides with the results of the present study.

Table 10. *Mean values of solution (VAc/ELO®=1/1, w/w) uptake before curing, wood WPG after the treatment (WPG$_t$), and wood ASE after 1st and 4th WS–OD cycles.*

Schedule	Uptake (kg m^{-3})	WPG$_t$ (%)	ASE (%)	
			Cycle 1	Cycle 4
1.25 bar (20 min)+2 bar (60 min)	109.0 (7.7)	8.6 (0.9)	37.7 (9.5)	39.5 (11.1)
2 bar (20 min)+4.5 bar (50 min)	180.2 (11.5)	13.6 (0.9)	35.1 (5.6)	39.6 (5.5)
0.5 bar (20 min)+4.5 bar (50 min)	373.8 (22.7)	22.6 (2.1)	38.9 (5.7)	42.1 (6.6)
vacuum (5 min)+5 bar (60 min)	610.3 (33.9)	37.1 (3.0)	43.6 (4.8)	46.5 (5.3)

3.2.3 Leaching test

Leaching tests by water and solvent (acetone) were performed on samples treated with VAc–ELO® (VA/ELO®=1:1, w/w) copolymer. Figure 15 shows the relationship between the initial WPG and P (*i.e.* percentage of copolymer left in wood after water leaching and Soxhlet extraction with acetone) for individual treated samples having less than 30% WPG.
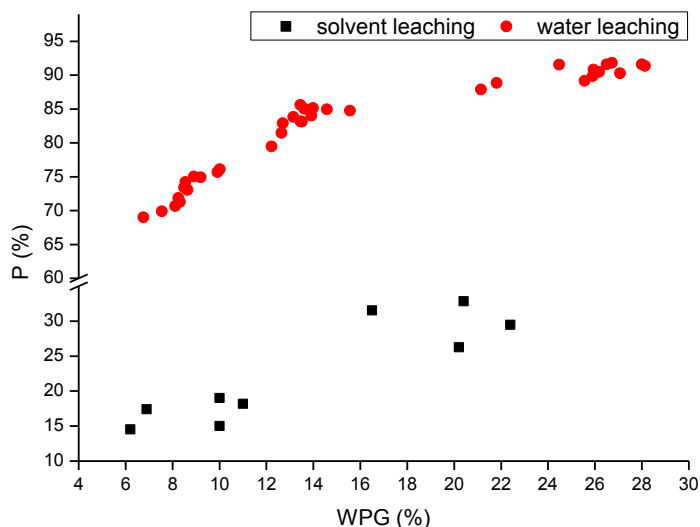
Figure 15. Relationship between initial WPG and P (percentage of VAc–ELO copolymer left in wood after water leaching and Soxhlet extraction by acetone).

The solubility of VAc–ELO® copolymer in water and various solvents was summarized in *Paper I*, which showed that the copolymer is soluble in organic solvents such as methanol, THF, acetone and acetonitrile, but not in water. As shown in Figure 15, after 7 h Soxhlet extraction by acetone, treated sample of 6.2% WPG has only about 15% impregnated copolymer remained inside the wood, while there is still approximately 30% copolymer left inside wood sample with 22.4% WPG. Wood samples after extraction were characterized

by ATR–FTIR (spectra not shown here). Compared to the spectra of samples before solvent extraction, the intensities of characteristic peaks of copolymer decrease but do not disappear, such as the stretching of C=O at 1740 cm^{-1}. As the VAc–ELO® copolymer is soluble in acetone, any copolymer remaining in wood after extraction is assumed to be chemically bound to the hydroxyl groups of the cell wall. However, for the copolymer located in the cell lumen, rays, and resin canals which are not chemically bound to the hydroxyl groups of the cell wall, it can be extracted from the wood by solvent.

Leaching by solvent does not simulate the environmental conditions in reality. A distribution of individual wood samples having various WPG were subjected to water leaching, and the impact of water leaching on the change of WPG is evaluated (Figure 15). After four cycles of leaching, more than 70% of the impregnated copolymers still remained in the wood. Samples with low WPG tend to leach more than those with high WPG. Since the formed copolymer is insoluble in water, most of the leached formulation in water comes presumably from the residue of impregnated agent on the wood surface.

3.2.4 Microscopy observations

After water leaching, treated samples were analysed by microscopy to confirm the success of the treatments. Sections from subsamples were cut from the core of the treated samples and visualised by light microscopy and SEM. Obtained images are shown in Figure 16 (*Paper III*). According to SEM observation, treated samples (28% WPG) after water leaching shows impregnated copolymer mainly in the resin canals, rays and occasionally in the cell lumens, especially in the tracheid cell lumens of latewood (Figure 15a–c). Copolymer residues precipitated in the inner cell wall are aligned in vertical direction to the unfilled tracheid lumens (Figure 16d). Some of the bordered pits on axial tracheids appear unfilled while others are sealed with copolymer (Figure 16e), which is presumably due to the aspiration of bordered pits during curing and the drying process. In Figure 16f, radial longitudinal section shows characteristic fractures running across the wood structure from the tracheid cell wall into the cell lumina. The nature of the perpendicular fractures provides evidence for penetration and copolymerization in the tracheid cell walls. It is presumed that the copolymer in the cell wall interacts with the hydroxyl groups of wood polymers. The change in the wood cell wall structure ensures great dimensional stability.
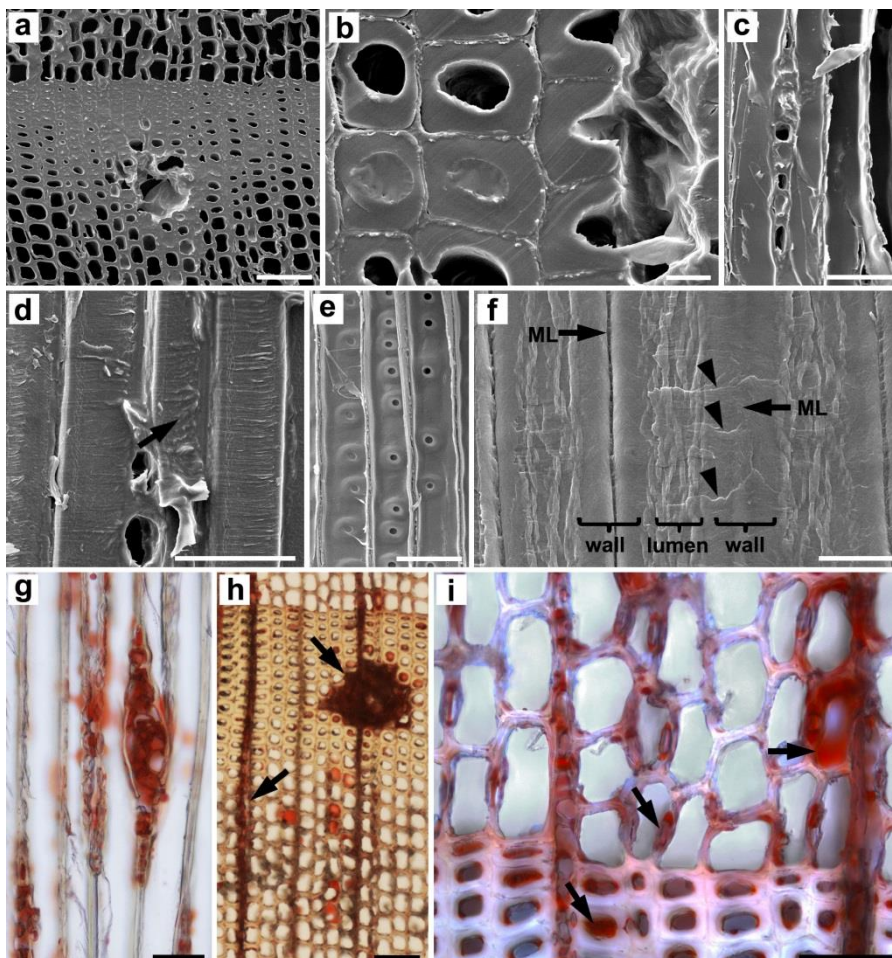
Figure 16. Micrographs of wood treated by VAc–ELO® (VAc/ELO®=1/1, w/w) copolymer. (a–f) SEM images; transverse section (a, b), tangential longitudinal section (c, d) and radial longitudinal section (e, f). (g–i) Light microscopy images after staining with Sudan III; tangential longitudinal section (g), and transverse section (h, i). Scale bars, 10 μm (b, f), 50 μm (c–e, g, i), and 100 μm (a, h). ML, middle lamella.

Light microscopy observations on treated samples (28% WPG) after staining with Sudan III confirm the presence of the copolymer in the rays, resin canals and occasionally in the cell lumina (Figure 16g–i). Some precipitates located in the bordered pits and inner cell walls of tracheids are also visible (Figure 16i). The filled rays and resin canals suggest the pathway for penetration of VA–ELO® solution into the wood is through the rays and resin canals.

50

3.2.5 Mechanical properties

Mechanical tests were performed on paired control and treated samples at five WPG levels (8–28%). The treated and control samples were conditioned separately in order to obtain samples with similar MC. Table 11 quantifies the difference by using paired t–test which compares the means of two independent groups to determine whether there is statistically significant difference between them. Treatment with VAc–ELO®, like most of the wood treatments, results in slight decrease in the mechanical properties compared to the corresponding untreated samples. By calculating the P values from the t test , the MOR, compression (∥) and hardness (⊥) show significant difference in the tested range, followed by the shear strength (∥) in which insignificant difference is observed only at the lowest WPG. With respect to MOE, compression (⊥) and hardness (∥), the difference between control and treated samples gradually increases as a result of increasing WPG. Due to the insufficient quantities of control samples, the impact bending strength of treated samples having different WPG were compared with only a group of control samples obtained from another batch. The impact bending strength of the treated samples is inferior to the control samples (results not shown here).

Table 11. *Comparison between VAc–ELO® (VAc/ELO®=1/1, w/w) treated and control samples with respect to mechanical properties (MOE, MOR, compression, hardness and shear).*

WPG	MOE		MOR		Comp. ∥		Comp. ⊥		Hardness ∥		Hardness ⊥		Shear ∥	
	p*	Δ%	p	Δ%	p	Δ%	p	Δ%	p	Δ%	p	Δ%	p	Δ%
8%	0.140	–5	**0.000**	–18	**0.000**	–19	**0.033**	–16	0.149	–6	**0.000**	–22	0.282	–7
13%	0.076	–9	**0.000**	–22	**0.000**	–19	0.093	–11	0.100	–9	**0.001**	–22	**0.012**	–17
18%	0.177	–7	**0.001**	–19	**0.000**	–17	0.091	–13	**0.004**	–18	**0.000**	–18	**0.000**	–28
22%	**0.023**	–12	**0.000**	–21	**0.000**	–17	**0.001**	–20	**0.021**	–17	**0.000**	–23	**0.001**	–15
28%	**0.002**	–10	**0.000**	–20	**0.000**	–16	**0.003**	–22	**0.001**	–16	**0.000**	–17	**0.000**	–23

*P values (calculated from t–test) and relative changes (Δ%) of the mechanical properties at five WPG levels. Values of $P < 0.05$ are shown in bold indicating significant difference between control and treated samples.

The reduction in mechanical performance of VAc–ELO® treated wood is comparable to that of ELO® treated wood, in which the largest difference in MOR was observed, followed by hardness (⊥) and compression (∥) for the ELO® treated wood (Jebrane *et al.*, 2015b). Moreover, in comparison to other types of treatments, it was reported that furfurylated wood showed significantly decreased impact bending strength but increased hardness with no obvious change for static bending properties (Epmeier *et al.*, 2004; Lande *et al.*, 2004b). In addition, investigations on acetylated wood did not show significant changes in MOR and MOE, while the hardness was either increased or

remained unchanged depending on the actual acetylation methods and degree of acetylation (Jebrane *et al.*, 2015b; Hill, 2007).

The observed decrease in the mechanical performance of VAc–ELO[®] treated wood could be attributed to many factors. For chemical modification, the impregnating agents remain and swell the cell wall to some extent, resulting in lesser lignocellulosic fibres per cross section than control wood contributing to reduced mechanical strength (Rowell, 1996). Additionally, it has been proven that when the oil front passes through the cell, the pressure gradient can alter the internal stress considerably, resulting in a localized cell wall damage in the ray region and damages in the S1 cell wall layers at any location where the oil front has passed, especially in the border between early– and latewood (Megnis *et al.*, 2002). The amount of impregnated copolymer in the cell wall determines the extent of impact on the mechanical properties. Consequently, treated samples of low WPG were expected to perform better than high WPG samples.

3.2.6 Durability

The impact of the VAc–epoxidzied LO treatment on wood decay resistance was evaluated by subjecting treated wood samples to fungal attack. Previous ^{1}H–NMR investigation showed that almost no signals corresponding to the oil moieties can be found after reaction of VAc–SO, VAc–ESO[®], VAc–partly epoxidized SO, and VAc–epoxidized LO with low epoxy content, therefore, the screening tests were preliminarily performed on wood treated with VAc–epoxidized LO with higher epoxy content (*i.e.* ELO[®]) which can form copolymers in wood (Table 12).

Table 12. *Screening test showing the ML of control and treated (VAc/oil=1:1, w/w) samples exposed to brown rot and white rot fungi for 9 weeks (standard deviations in parentheses).*

Samples	WPG	*Trametes versicolor*	*Postia placenta*	*Gloeophyllum trabeum*	*Coniophora puteana*
Control	-	13.7 (5.2)	46.1 (6.6)	27.1 (6.4)	33 (2.9)
VAc–ELO2	37.6 (6.0)	6.9 (2.9)	22.4 (11.2)	17.6 (6.6)	18.3 (2.8)
VAc–ELO1	35.1 (4.0)	6.4 (3.8)	23.8 (15.6)	14.3 (3.3)	18.8 (11.7)
VAc–ELO[®]	49.4 (3.3)	3.7 (1.9)	21.2 (7.3)	14.1 (4.1)	10.2 (5.8)

Note: values of ML represent means of 12 replicates.

Initially, the mixture of VAc and ELO[®] in aqueous phase were emulsified by non–ionic emulsifier Brij[®] S 100 (average M_n equals 4.670 g mol^{−1}) and then impregnated into the wood samples. Brij[®] S 100 used in the screening test was found to retain stable emulsion; however, due to the high molecular weight of

Brij® S 100, the obtained emulsions were highly viscous which limited the penetration of the impregnating agents into the wood cell wall. In addition, the granular form of Brij® S 100 was difficult to dissolve in aqueous solution at room temperature and contributed significantly to the high viscosity of the formulation. As shown in Table 12, the treated samples show improved resistance to fungal attack, especially the VAc–ELO® treated wood in comparison to the durability of control samples. Moreover, samples after treatment show better decay resistance to the white rot fungus (*Trametes versicolor*) than the brown rot fungi (*Postia placenta, Gloeophyllum trabeum, Coniophora puteana*). Nevertheless, the treatment in presence of Brij® S 100 cannot provide sufficient protection according to standard EN 113 (1996) which requires less than 3% ML.

The screening test in Table 12 shows that the effect of epoxy content on the durability of treated samples is not significant, which forces a study on the role and effect of various emulsifiers on the decay resistance of treated samples. The conventional method for VAc emulsion polymerization uses potassium persulfate as initiator and sodium lauryl sulfate (SDS) as emulsifier (Erbil, 2000). However, the application of SDS failed to perform as an effective emulsifier in the VAc-oil-H_2O formulation, even used at high concentration. Alternatively, Brij® S 100 was substituted by a combination of emulsifiers CTAB and span® 80 at low concentration. CTAB is well known as an efficient compound used in household products such as shampoos and cosmetics. CTAB (2.6%, w/w) combined with Span® 80 (1.6%, w/w) can stabilize VAc–oil–H_2O formulation for several days. Compared to Brij® S 100 (3.0%, w/w), the use of CTAB and Span® 80 can substantially decrease the viscosity of the solution, facilitating the impregnation of the emulsion into the wood.

Table 13 shows the ML of control and treated wood samples at three WPG after 16 weeks exposure to white– (*Trametes versicolor*) and brown rot fungi (*Lentinus lepideus, Postia placenta* and *Coniophora puteana*) in accordance to the standard EN 84 (1997) and EN 113 (1996). Brown rot fungus *Gloeophyllum trabeum* used in the screening test was replaced by *Lentinus lepideus* which is recommended in the standard for testing of oil-based formulations. The MC of the samples after the test was in line with the requirements of the standard (MC in the range 25–80%). The mixtures here were emulsified by CTAB and Span® 80 instead of previously used Brij® S 100. As shown in the Table, the ML of treated samples decreases with increase of WPG, and the durability of treated samples is significantly improved compared to control samples. Apart from *Lentinus lepideus*, control samples lost more than 20% of their mass after 16 weeks of fungal exposure, which was assumed to be valid according to the requirement described in the standard EN

113 (1996). The fungal resistance can be quantified by the calculated DC. Durability of untreated scots pine sapwood is classified as DC 5 (non–durable) according to the standard EN 350–2 (1994). Since the ML of treated samples of 5% WPG against *Trametes versicolor* was 8.1%, their protection provided for the wood was inadequate (DC 3) according to the EN 113 (1996). Treated samples of 8% WPG were sufficient to inhibit the fungal growth, which led to DC 2.

Table 13. *ML of control and VAc–ELO® treated (VAc/ELO®=1/1, w/w) samples (5, 8 and 13% WPG) exposed to brown– and white rot fungi for 16 weeks according to standard EN 113 (standard deviations in parentheses).*

WPG		ML (%) after fungal exposure and calculated durability class (DC)				
		Trametes versicolor	*Lentinus lepideus*	*Postia placenta*	*Coniophora puteana*	DC
5%	Treated	8.1 (2.7)	2.1 (1.3)	0.3 (0.1)	1.3 (0.5)	3
	Control	23.4 (3.3)	13.2 (4.8)	58.2 (1.5)	51.4 (7.0)	
8%	Treated	4.4 (2.5)	-0.5 (0.5)	-0.9 (0.9)	1.1 (0.2)	2
	Control	25.1 (2.9)	15.5 (8.3)	59.4 (2.3)	55.9 (7.7)	
13%	Treated	0.1 (1.9)	-0.7 (0.6)	-2.3 (0.4)	-1.0 (0.7)	1
	Control	24.7 (3.8)	20.8 (3.6)	59.5 (1.3)	53.9 (4.0)	

Note: values of ML represent means of 4 replicates.

The substitution of CTAB and Span® 80 for Brij® S 100 increases the emulsion stability and reduces the viscosity of the emulsion, which makes impregnation more viable. Due to the slightly alkaline character of CTAB, it is presumed that the emulsifier CTAB can catalyze the reaction between ELO®'s epoxide groups and the hydroxyl groups of the wood by ring opening of epoxide groups. On the other hand, compared to wood treated with plant oil (e.g. ELO® and LO) at low retention (Terziev & Panov, 2011), the durability of wood treated with the VAc–ELO® copolymer is significantly improved according to standard EN 113 (1996), even at relatively low WPG of 8%.

4   Additional study on furfuryl alcohol–ELO$^{®}$ treated wood

As a complement to VAc–plant oil treated wood, the synthesis and characterization of furfuryl alcohol–ELO$^{®}$ treated wood was also explored (*Paper VI*). Since both the furfuryl alcohol (FA) and ELO$^{®}$ are derived from renewable resource, the copolymerization of FA and ELO$^{®}$ can produce a fully bio–based polymer which combines the virtues of ELO$^{®}$'s flexibility and rigidity of poly furfuryl alcohol (Pin *et al.*, 2015).

Wood blocks with dimensions 23×23×35 mm were prepared for leaching, dimensional stability and durability tests, while stakes of 20×20×340 mm were prepared for the mechanical tests. Formulations of FA–ELO$^{®}$ (1:1, v:v) catalysed by maleic anhydride (2%) were mixed and then wood blocks and stakes impregnated together in a stainless–steel reactor with process consisting of 5 min vacuum (80%) and 30 min pressure (5 bars). Samples after impregnation were kept in sealed containers and cured at 70°C for 2 weeks. Subsequently, four cycles of WS–OD were performed on treated wood blocks to evaluate the dimensional stability and leachability.

Table 14. *The WPG, dimensional stability and leaching resistance of FA–ELO$^{®}$ treated wood blocks, and WPG of FA–ELO$^{®}$ treated wood stakes (standard deviations in parentheses).*

Treatment	Wood blocks			Wood stakes
	WPG (%)	ASE (%)	P (%)	WPG (%)
FA–ELO$^{®}$	59.7 (8.4)	43.1 (3.7)	94.8 (0.8)	26.4 (8.2)

After 4 cycles of WS–OD, FA–ELO$^{®}$ treated wood of 59.7% WPG shows great leaching resistance (P=94.8%, *i.e.* 94.8 % of polymer remained in wood after leaching by water) and dimensional stability (ASE=43.1%, Table 14). However, the dimensional stability of FA–ELO$^{®}$ treated wood is inferior to the only FA treated wood which showed that 32%–47% WPG can result in 60–

70% ASE (Epmeier *et al.*, 2004). Esteves *et al.* (2011) also reported that almost 45% ASE (measured in the radial direction) can be obtained for furfurylated wood with 38% WPG.

Table 15. *Mechanical properties of FA–ELO® treated (26.4% WPG) and control samples (standard deviations in parentheses).*

Mechanical properties	FA–ELO®	Control
Impact bending strength (kJ m^{-2})	61.5 (5.8)	48.5 (4.4)
Modulus of elasticity (N mm^{-2})	12702.6 (2011.5)	12987.0 (1706.4)
Brinell hardness	1.7 (0.3)	1.4 (0.1)

The mechanical properties of wood after FA–ELO® treatment are shown in Table 15. The changes in MOE are not significant, which is in line with that of FA treated wood (Esteves *et al.*, 2011). However, the impact bending strength increased by 30% for FA-ELO® treatment at 26.4% WPG, while Lande *et al.* (2004b), indicated a 53–57% decrease in impact strength for merely FA treated wood of 32–47% WPG. The change in Brinell hardness for FA–ELO® treated wood is comparable to that of FA treated wood. According to Table 15, the hardness of FA–ELO® treated wood increases by 21% at 26.4% WPG. Lande *et al.* (2004b) reported that FA treated wood (*Pinus sylvestris* L.*)* with 32–47% WPG brought about 17–30% increase in hardness, which is in line with the results of Esteves *et al.* (2011) who reported a 55.7% increase in hardness of *Pinus pinaster* wood caused by furfurylation (38% WPG). However, high hardness is associated with high brittleness, which is not always favourable for some applications.

Table 16. *ML of FA–ELO® treated samples (59.7% WPG) against 3 decay fungi according to EN 113 (standard deviations in parentheses).*

Fungus		ML (%) and calculated durability class (DC)		
		Control	FA–ELO®	DC
Brown rot	*Postia placenta*	34.3 (2.4)	4.0 (2.2)	1
	Coniophora puteana	42.4 (3.0)	2.7 (1.2)	1
White rot	*Trametes versicolor*	18.7 (2.7)	2.0 (0.2)	1

Note: values of ML represent means of 4 replicates.

Table 16 shows the ML and DC of FA–ELO® treated wood block against brown– and white rot fungi. In comparison to the control samples, the fungal growth on the treated samples is substantially inhibited. The DC for the FA–ELO® treated wood is calculated according to standard EN 350–1 (1994). The DC of treated samples exposed to the white rot- and brown rot fungi are

regarded as class 1, which is considered to be very durable. Similar durability results were reported in the literature using the furfurylation process by which an increased resistance to white– and brown rot decay was documented (Esteves *et al.*, 2011). The authors found that the ML of furfurylated *Pinus pinaster* wood (38% WPG) exposed to *Postia placenta* and *Coniophora puteana* decreased to 1.11% and 0.78% respectively. Likewise, Lande *et al.* (2004b) showed the ML of the furfurylated *Pinus sylvestris* wood (75% WPG) caused by *P. placenta* decreased to 4.3%, compared to ML of 60% for untreated samples.

5   Conclusions

Although studied for more than 50 years, wood modification has limited industrial application as both methods and treated volumes of timber. Modified wood competes with wood impregnated with copper–based preservatives that offer reliable performance and significantly lower cost of the product. The above has been the driving force of the entire study aiming at developing a wood modification method that fulfils several criteria. It was desirable the origin of the precursors to be bio–based products that are renewable, abundant and cheap. Another criterion was to use already existing techniques and technologies to facilitate eventual practical implementation of the study results. The modified wood was expected to demonstrate improved dimensional stability, increased durability against biological degradation but retaining the mechanical properties of the untreated material.

The present study developed a novel method of combining plant oil and vinyl acetate (VAc) as impregnation agents for wood modification and protection. Linseed oil (LO) and soybean oil (SO) were *in–situ* epoxidized with hydrogen peroxide and AA in the presence of concentrated sulfuric acid. By controlling the reaction time during the epoxidation process, the epoxidized oils with various epoxy content were prepared and analysed by means of ^{1}H–NMR to quantify the number of epoxy groups in oil and to determine the degree of epoxidation.

LO epoxidised to maximum degree was found to be the most reactive monomer among other oils studied here in copolymerization with VAc, and the VAc–ELO® combination was chosen as target formulation to be studied extensively. ^{13}C–NMR was employed to reveal the chemical structure of VAc–ELO® copolymer. A new chain connection between oil molecule and the PVAc chain with new signals at 31.0 and 15.3 ppm emerged which are attributable to the carbons of ELO®–CH–CH–PVAc linkage. DSC proved the formation of VAc–ELO® copolymer with single glass transition temperature (T_g) appeared

at approximately 25°C in thermogram upon heating. For the VAc–ELO® combination, the yield of reaction was found to increase with increasing VAc/ELO® ratio, reaction time, temperature and catalyst amount. Although the feed ratio VAc/ELO®=3/1 gives the highest yield (91.3%) compared to the feed ratio of 1/1 (54.3%) and 1/3 (24.4%), the feed ratio of VAc/ELO®=1/1 was chosen by taking into account the low cost and eco–friendly nature of ELO®.

Previous drawbacks of using ELO® for wood modification (e.g. immediate polymerization initiation after mixing with catalyst acetic acid (AA), and corrosion caused by the AA) have been overcame by the proposed method. VAc–plant oil treated wood avoids the demand for AA and the copolymerization process starts only upon curing, which increases the maintainability of the process. As necessary ingredients of the modification formulation, two surface–active agents namely, CTAB and Span® 80 at low concentration were employed to emulsify the immiscible VAc and ELO® monomers in water. Due to the slightly alkaline character of CTAB, it is presumed that the emulsifier CTAB can catalyse the reaction between ELO® and the hydroxyl groups of wood by ring opening of epoxide of ELO®.

One of the key moments in the study was to find out and optimise the curing parameters after impregnation of wood. The curing process in wood was monitored using ATR–FTIR by measuring the areas under characteristic peaks at 1650 cm^{-1} and 1509 cm^{-1} which correspond to the C=C stretching in the unreacted VAc monomer and the aromatic skeletal vibration of lignin respectively. The increasing curing temperature and duration resulted in decreased peak area ratio A_{1650}/A_{1509} due to the consumption of VAc monomers during curing. Improved dimensional stability of wood after drying was also observed with increase of curing temperature and duration, while the WPG obtained at the studied curing temperatures and durations were not significantly different. From the economic point of view, the VAc–ELO® treated wood cured at 90°C for 168 h was considered as an optimal condition, which contributed to 42.1% ASE after water soaking and oven drying. Moreover, it was found that VAc–ELO® treated wood with increased WPG does not correlate with ASE.

The VAc–ELO® treated wood showed great leaching resistance to water, and the small amount of leached formulation in water presumably came from the residue of impregnated agent residing on the wood surface. The impregnated copolymer in the wood was mainly presented in rays, resin canals and occasionally in tracheid cell lumens, which suggests the pathway for penetration of VA–ELO® solution into the wood through rays and resin canals. Most of the impregnated copolymer can be leached from the wood after

solvent extraction. The remaining copolymer in wood after solvent extraction was assumed to be chemically bound to the hydroxyl groups of the wood cell wall.

Like most of the wood treatments, the mechanical properties of untreated wood performed slightly better than those of the corresponding treated wood, especially for the MOR, compression (∥) and hardness (⊥), and the difference between control and treated samples gradually increases as a result of increasing WPG. The protective effectiveness of VAc–ELO® treated wood at different WPG against white rot– (*T. versicolor*) and brown rot fungi (*L. lepideus*, *P. placenta* and *C. puteana*) showed that treated samples of 8% WPG is enough to ensure decay resistance against these test fungi (durability class 2), which was suggested to protect wood in above ground applications.

Besides VAc–ELO® treated wood, another application explored was to combine ELO® with furfuryl alcohol (FA). Because both FA and ELO® are derived from renewable resources, the copolymerization of FA and ELO® can produce a fully bio–based polymer which combines the virtues of ELO's flexibility and rigidity of poly furfuryl alcohol. The FA–ELO® treated wood showed great leaching resistance to water, improved dimensional stability and durability compared to untreated samples.

References

Adhvaryu, A. & Erhan, S. (2002). Epoxidized soybean oil as a potential source of high–temperature lubricants. *Industrial Crops and Products,* 15(3), pp. 247–254.

Allegretti, O., Brunetti, M., Cuccui, I., Ferrari, S., Nocetti, M. & Terziev, N. (2012). Thermo–vacuum modification of spruce (*Picea abies Karst.*) and fir (*Abies alba* Mill.) wood. *BioResources,* 7(3), pp. 3656–3669.

Biermann, C.J. (1993). *Essentials of pulping and papermaking*: Academic press.

Boonstra, M.J., Van Acker, J., Tjeerdsma, B.F. & Kegel, E.V. (2007). Strength properties of thermally modified softwoods and its relation to polymeric structural wood constituents. *Annals of Forest Science*, 64(7), pp. 679–690.

Caillol, S., Desroches, M., Boutevin, G., Loubat, C., Auvergne, R. & Boutevin, B. (2012). Synthesis of new polyester polyols from epoxidized vegetable oils and biobased acids. *European Journal of Lipid Science and Technology,* 114(12), pp. 1447–1459.

Campanella, A., Fontanini, C. & Baltanas, M.A. (2008). High yield epoxidation of fatty acid methyl esters with performic acid generated *in situ*. *Chemical Engineering Journal,* 144(3), pp. 466–475.

Campanella, A., Rustoy, E., Baldessari, A. & Baltanás, M.A. (2010). Lubricants from chemically modified vegetable oils. *Bioresource Technology,* 101(1), pp. 245–254.

Clark, A.J. & Hoong, S.S. (2014). Copolymers of tetrahydrofuran and epoxidized vegetable oils: application to elastomeric polyurethanes. *Polymer Chemistry,* 5(9), pp. 3238–3244.

Deka, M. & Saikia, C. (2000). Chemical modification of wood with thermosetting resin: effect on dimensional stability and strength property. *Bioresource Technology,* 73(2), pp. 179–181.

Dinda, S., Patwardhan, A.V., Goud, V.V. & Pradhan, N.C. (2008). Epoxidation of cottonseed oil by aqueous hydrogen peroxide catalysed by liquid inorganic acids. *Bioresource Technology,* 99(9), pp. 3737–3744.

Dubey, M.K., Pang, S. & Walker, J. (2012). Oil uptake by wood during heat–treatment and post–treatment cooling, and effects on wood dimensional stability. *European Journal of Wood and Wood Products,* 70(1), pp. 183–190.

Epmeier, H., Johansson, M., Kliger, R. & Westin, M. (2007). Material properties and their interrelation in chemically modified clear wood of Scots pine. *Holzforschung,* 61(1), pp. 34–42.

Epmeier, H., Westin, M. & Rapp, A. (2004). Differently modified wood: Comparison of some selected properties. *Scandinavian Journal of Forest Research,* 19(suppl. 5), pp. 31–37.

Eranna, P.B. & Pandey, K.K. (2012). Solvent–free chemical modification of wood by acetic and butyric anhydride with iodine as catalyst. *Holzforschung*, 66(8), 967–971.

Erbil, Y.H. (2000). *Vinyl acetate emulsion polymerization and copolymerization with acrylic monomers*: CRC press.

Esteves, B., Nunes, L. & Pereira, H. (2011). Properties of furfurylated wood (*Pinus pinaster*). *European Journal of Wood and Wood Products,* 69(4), pp. 521–525.

Esteves, B. & Pereira, H. (2008). Wood modification by heat treatment: A review. *BioResources,* 4(1), pp. 370–404.

European Standard EN 113 (1996). Wood perservatives–test method for determining the protective effectiveness against wood destroying basidiomycetes–determination of toxic values.

European Standard EN 350–1 (1994). Durability of Wood and Wood–based Products – natural Durability of Solid Wood: Guide to the principles of testing and classification of the natural durability of wood.

European Standard EN 350–2 (1994). Durability of wood and woodbased products–natural durability of solid wood–Part 2: Guide to natural durability and treatability of selected wood species of importance in Europe.

European Standard EN 84 (1997). Wood preservatives–accelerated ageing of treated wood prior to biological testing–leaching procedure.

Evans, P.D., Wingate–Hill, R. & Cunningham, R.B. (2009). Wax and oil emulsion additives: How effective are they at improving the performance of preservative–treated wood? *Forest Products Journal,* 59(1/2), pp. 66–70.

Farias, M., Martinelli, M. & Bottega, D.P. (2010). Epoxidation of soybean oil using a homogeneous catalytic system based on a molybdenum (VI) complex. *Applied Catalysis A: General,* 384(1), pp. 213–219.

Gamauf, C., Metz, B. & Seiboth, B. (2007). Degradation of Plant Cell Wall Polymers by Fungi. *In Environmental and Microbial Relationship:* Springer.

Glasser, W.G. & Jain, R.K. (1993). Lignin derivatives. I. alkanoates. *Holzforschung,* 47(3), pp. 225–233.

Goldstein, I. (1955). The impregnation of wood to impart resistance to alkali and acid. *Forest Products Journal,* 5(4), pp. 265–267.

Grishchuk, S. & Karger–Kocsis, J. (2011). Hybrid thermosets from vinyl ester resin and acrylated epoxidized soybean oil (AESO). *Express Polymer Letters,* 5(1), pp. 2–11.

Guo, A., Cho, Y. & Petrović, Z.S. (2000). Structure and properties of halogenated and nonhalogenated soy-based polyols. *Journal of Polymer Science Part A: Polymer Chemistry,* 38(21), pp. 3900–3910.

Hill, C.A. (2007). *Wood modification: chemical, thermal and other processes*: John Wiley & Sons.

Humar, M. & Lesar, B. (2013). Efficacy of linseed–and tung–oil–treated wood against wood–decay fungi and water uptake. *International Biodeterioration & Biodegradation,* 85, pp. 223–227.

Hyvönen, A., Piltonen, P. & Niinimäki, J. (2006). Tall oil/water–emulsions as water repellents for Scots pine sapwood. *Holz als Roh–und Werkstoff,* 64(1), pp. 68–73.

Hyvönen, A., Nelo, M., Piltonen, P. & Niinimäki, J. (2007). Using the emulsion technique and an iron catalyst to enhance the wood protection properties of tall oil. *Holz als Roh– und Werkstoff*, 65(3), pp. 247–249.

International Standard ISO 3129 (1975). Wood–sampling methods and general requirements for physical and mechanical tests.

International Standard ISO 3132 (1975). Wood–testing in compression perpendicular to grain.

International Standard ISO 3133 (1975). Wood–determination of ultimate strength in static bending.

International Standard ISO 3347 (1976). Wood–determination of ultimate shearing stress parallel to grain.

International Standard ISO 3348 (1975). Wood–determination of impact bending strength.

International Standard ISO 3349 (1975). Wood–determination of modulus of elasticity in static bending.

International Standard ISO 3350 (1975). Wood–determination of static hardness.

International Standard ISO 3787 (1976). Wood–test methods–determination of ultimate stress in compression parallel to grain.

Jebrane, M., Fernández–Cano, V., Panov, D., Terziev, N. & Daniel, G. (2015a). Novel hydrophobization of wood by epoxidized linseed oil. Part 1. Process description and anti–swelling efficiency of the treated wood. *Holzforschung,* 69(2), pp. 173–177.

Jebrane, M., Fernández–Cano, V., Panov, D., Terziev, N. & Daniel, G. (2015b). Novel hydrophobization of wood by epoxidized linseed oil. Part 2. Characterization by FTIR spectroscopy and SEM, and determination of mechanical properties and field test performance. *Holzforschung,* 69(2), pp. 179–186.

Jebrane, M., Pichavant, F. & Sèbe, G. (2011). A comparative study on the acetylation of wood by reaction with vinyl acetate and acetic anhydride. *Carbohydrate Polymers,* 83(2), pp. 339–345.

Jebrane, M. & Sebe, G. (2007). A novel simple route to wood acetylation by transesterification with vinyl acetate. *Holzforschung,* 61(2), pp. 143–147.

Jensen, E.S., Gatenholm, P. & Sellitti, C. (1992). An ATR-FTIR study on penetration of resins in wood. *Die Angewandte Makromolekulare Chemie,* 200(1), pp. 77–92.

Klüppel, A. & Mai, C. (2013). The influence of curing conditions on the chemical distribution in wood modified with thermosetting resins. *Wood Science and Technology,* 47(3), pp. 643–658.

Kollmann, F. & Fengel, D. (1965). Änderungen der chemischen Zusammensetzung von Holz durch thermische Behandlung. *Holz als Roh- und Werkstoff,* 23(12), pp. 461–468.

Koski, A. (2008). Applicability of crude tall oil for wood protection. *Doctoral thesis*, University of Oulu, Finland, ISBN 978–951–42–8722–0.

Kumar, S., Dev, I. & Singh, S. (1991). Hygroscopicity and dimensional stability of wood acetylated with thioacetic acid and acetyl chloride. *Journal of the Timber Development Association of India,* 37(1), pp. 25–32.

Laidlaw, R., Pinion, L. & Smith, G. (1967). Dimensional Stabilisation of Wood II. Grafting of vinyl polymers to wood components. *Holzforschung,* 21(4), pp. 97–102.

Lande, S., Eikenes, M. & Westin, M. (2004a). Chemistry and ecotoxicology of furfurylated wood. *Scandinavian Journal of Forest Research,* 19(suppl. 5), pp. 14–21.

Lande, S., Westin, M. & Schneider, M. (2004b). Properties of furfurylated wood. *Scandinavian Journal of Forest Research,* 19(suppl. 5), pp. 22–30.

Larock, R.C., Dong, X., Chung, S., Reddy, C.K. & Ehlers, L.E. (2001). Preparation of conjugated soybean oil and other natural oils and fatty acids by homogeneous transition metal catalysis. *Journal of the American Oil Chemists' Society,* 78(5), pp. 447–453.

Li, F., Hanson, M. & Larock, R. (2001). Soybean oil–divinylbenzene thermosetting polymers: synthesis, structure, properties and their relationships. *Polymer,* 42(4), pp. 1567–1579.

Li, F., Hasjim, J. & Larock, R.C. (2003). Synthesis, structure, and thermophysical and mechanical properties of new polymers prepared by the cationic copolymerization of corn oil, styrene, and divinylbenzene. *Journal of Applied Polymer Science,* 90(7), pp. 1830–1838.

Li, F. & Larock, R.C. (2000). Thermosetting polymers from cationic copolymerization of tung oil: synthesis and characterization. *Journal of Applied Polymer Science,* 78(5), pp. 1044–1056.

Li, F. & Larock, R.C. (2001). New soybean oil–styrene–divinylbenzene thermosetting copolymers. I. Synthesis and characterization. *Journal of Spplied Polymer Science,* 80(4), pp. 658–670.

Li, F. & Larock, R.C. (2003). Synthesis, structure and properties of new tung oil–styrene–divinylbenzene copolymers prepared by thermal polymerization. *Biomacromolecules,* 4(4), pp. 1018–1025.

Li, J.–Z., Furuno, T., Zhou, W.R., Ren, Q., Han, X.Z. & Zhao, J.–P. (2009). Properties of acetylated wood prepared at low temperature in the presence of catalysts. *Journal of Wood Chemistry and Technology,* 29(3), pp. 241–250.

Megnis, M., Olsson, T., Varna, J. & Lindberg, H. (2002). Mechanical performance of linseed oil impregnated pine as correlated to the take–up level. *Wood Science and Technology,* 36(1), pp. 1–18.

Meier, M.A., Metzger, J.O. & Schubert, U.S. (2007). Plant oil renewable resources as green alternatives in polymer science. *Chemical Society Reviews*, 36(11), pp. 1788–1802.

Militz, H. & Lande, S. (2009). Challenges in wood modification technology on the way to practical applications. *Wood Material Science and Engineering,* 4(1–2), pp. 23–29.

Nicholas, D. D. (1982). *Wood deterioration and its prevention by preservative treatments: Degradation and Protection of Wood* : Syracuse University Press.

Nordstierna, L., Lande, S., Westin, M., Karlsson, O. & Furo, I. (2008). Towards novel wood–based materials: chemical bonds between lignin–like model molecules and poly (furfuryl alcohol) studied by NMR. *Holzforschung,* 62(6), pp. 709–713.

Odian, G. (2004). *Principles of Polymerization*: John Wiley & Sons.

Olsson, T., Megnis, M., Varna, J. & Lindberg, H. (2001). Measurement of the uptake of linseed oil in pine by the use of an X–ray microdensitometry technique. *Journal of Wood Science,* 47(4), pp. 275–281.

Oyman, Z., Ming, W. & Van der Linde, R. (2005). Oxidation of drying oils containing non–conjugated and conjugated double bonds catalyzed by a cobalt catalyst. *Progress in Organic Coatings,* 54(3), pp. 198–204.

Panov, D., Terziev, N. & Daniel, G. (2010). Using plant oils as hydrophobic substances for wood protection. In: *Proceedings of 41st Annual Meeting of the International Research Group on Wood Protection,* Biarritz, France.

Patel, R., Dadida, C., Sarker, K. & Sen, D.J. (2015). Sudan dyes as lipid soluble aryl–azo naphthols for microbial staining. *European Journal of Pharmaceutical and Medical Research*, 2, pp. 417–425.

Petrie, E.M. (2007). Improving the moisture and heat resistance of PVAc wood adhesives. *Special Chem Adhesives and Sealants, Formulation Bulletin April,* 25.

Petrović, Z.S. (2008). Polyurethanes from vegetable oils. *Polymer Reviews,* 48(1), pp. 109–155.

Pilgård, A., Treu, A., Van Zeeland, A.N., Gosselink, R.J. & Westin, M. (2010). Toxic hazard and chemical analysis of leachates from furfurylated wood. *Environmental Toxicology and Chemistry,* 29(9), pp. 1918–1924.

Pin, J.M., Guigo, N., Vincent, L., Sbirrazzuoli, N. & Mija, A. (2015). Copolymerization as a strategy to combine epoxidized linseed oil and furfuryl alcohol: The design of a fully bio-based thermoset. *ChemSusChem,* 8(24), pp. 4149–4161.

Robinson, T.J., Via, B.K., Fasina, O., Adhikari, S. & Carter, E. (2011). Impregnation of bio–oil from small diameter pine into wood for moisture resistance. *BioResources,* 6(4), pp. 4747–4761.

Rowell, R.M. (2012). Chemical modification of wood to produce stable and durable composites. *Cellulose Chemistry and Technology,* 46(7–8), pp. 443–448.

Rowell, R.M. (1996). Physical and mechanical properties of chemically modified wood. In *Chemical Modification of Lignocellulosic Materials:* Marcel Dekker.

Rowell, R.M. (2005). 14 Chemical Modification of Wood. In *Handbook of Wood Chemistry and Wood Composites,* CRC press.

Sailer, M. & Rapp, A. (2001). Use of vegetable oils for wood protection. In: Proceedings of COST Action E22: *Environmental optimisation of wood protection*. Conference in Rinbek, Germany.

Saithai, P., Lecomte, J., Dubreucq, E. & Tanrattanakul, V. (2013). Effects of different epoxidation methods of soybean oil on the characteristics of acrylated epoxidized soybean oil–co–poly (methyl methacrylate) copolymer. *Express Polymer Letter* 7, pp. 910–924.

Salvini, A., Saija, L., Finocchiaro, S., Gianni, G., Giannelli, C. & Tondi, G. (2009). A new methodology in the study of PVAc-based adhesive formulations. *Journal of Applied Polymer Science,* 114(6), pp. 3841–3854.

Salvini, A., Saija, L., Lugli, M., Cipriani, G. & Giannelli, C. (2010). Synthesis of modified poly (vinyl acetate) adhesives. *Journal of Adhesion Science and Technology,* 24(8–10), pp. 1629–1651.

Saurabh, T., Patnaik, M., Bhagt, S. & Renge, V. (2011). Epoxidation of vegetable oils: a review. *International Journal of Advanced Engineering Technology,* 2, pp. 491–501.

Scheffer, T.C. (1966). Natural resistance of wood to microbial deterioration. *Annual Review of Phytopathology,* 4(1), pp. 147–168.

Schneider, M. (1995). New cell wall and cell lumen wood polymer composites. *Wood Science and Technology,* 29(2), pp. 121–127.

Schuchardt, U., Sercheli, R. & Vargas, R. M. (1998). Transesterification of vegetable oils: a review. *Journal of the Brazilian Chemical Society,* 9(3), pp. 199–210.

Schultz, T. & Glasser, W. (1986). Quantitative structural analysis of lignin by diffuse reflectance Fourier transform infrared spectrometry. *Holzforschung,* 40(suppl.), pp. 37–44.

Sharma, V. & Kundu, P. (2006). Addition polymers from natural oils—a review. *Progress in Polymer Science,* 31(11), pp. 983–1008.

Temiz, A., Akbas, S., Panov, D., Terziev, N., Alma, M.H., Parlak, S. & Kose, G. (2013a). Chemical composition and efficiency of bio–oil obtained from giant cane (*Arundo donax* L.) as a wood preservative. *BioResources,* 8(2), pp. 2084–2098.

Temiz, A., Kose, G., Panov, D., Terziev, N., Alma, M.H., Palanti, S. & Akbas, S. (2013b). Effect of bio-oil and epoxidized linseed oil on physical, mechanical, and biological properties of treated wood. *Journal of Applied Polymer Science,* 130(3), pp. 1562–1569.

Terziev, N. & Panov, D. (2011). Plant oils as "green" substances for wood protection. *Minimising the Environmental Impact of the Forest Products Industries*, pp. 143-149.

Ulvcrona, T., Flæte, P.O. & Alfredsen, G. (2012). Effects of lateral wood zone on brown rot resistance of untreated and linseed oil–impregnated Scots pine wood. *European Journal of Wood and Wood Products,* 70(5), pp. 771–773.

Van Eckeveld, A. (2001). *Natural oils as water repellents for scots pine*. Wageningen University, Thesis AV 2001-15, Wageningen.

Van Eckeveld, A., Homan, W. & Militz, H. (2001a). Increasing the water repellency of Scots pine sapwood. *Holzforschung und Holzverwertung,* 6, pp. 113–115.

Van Eckeveld, A., Homan, W. & Militz, H. (2001). Water repellency of some natural oils. In: Proceedings of COST Action E22: *Environmental optimisation of wood protection*. Conference in Rinbek, Germany.

Warwel, S. (1999). Complete and partial epoxidation of plant oils by lipase–catalyzed perhydrolysis. *Industrial Crops and Products,* 9(2), pp. 125–132.

Win, D.T. (2005). Furfural–gold from garbage. *Au Journal of Technolgy,* 8, pp. 185–190.

Windeisen, E., Bächle, H., Zimmer, B. & Wegener, G. (2009). Relations between chemical changes and mechanical properties of thermally treated wood. *Holzforschung,* 63(6), pp. 773–778.

Xia, W., Budge, S.M. & Lumsden, M.D. (2015). New ^{1}H NMR–Based Technique To Determine Epoxide Concentrations in Oxidized Oil. *Journal of Agricultural and Food Chemistry,* 63(24), pp. 5780–5786.

Xia, Y. & Larock, R.C. (2010). Vegetable oil–based polymeric materials: synthesis, properties, and applications. *Green Chemistry,* 12(11), pp. 1893–1909.

Yasuda, R. & Minato, K. (1994). Chemical modification of wood by non–formaldehyde cross–linking reagents. *Wood Science and Technology,* 28(2), pp. 101–110.

Yuan, J., Hu, Y., Li, L. & Cheng, F. (2013). The mechanical strength change of wood modified with DMDHEU. *BioResources,* 8(1), pp. 1076–1088.

Zhan, M. & Wool, R.P. (2010). Biobased composite resins design for electronic materials. *Journal of Applied Polymer Science,* 118(6), pp. 3274–3283.

Zhang, Y., Gu, J., Tan, H., Shi, J., Di, M., Zuo, Y. & Qiu, S. (2013). Preparation and characterization of film of poly vinyl acetate ethylene copolymer emulsion. *Applied Surface Science,* 276, pp. 223–228.

Zlatanić, A., Lava, C., Zhang, W. & Petrović, Z.S. (2004). Effect of structure on properties of polyols and polyurethanes based on different vegetable oils. *Journal of Polymer Science Part B: Polymer Physics,* 42(5), pp. 809–819.

Acknowledgments

I remember when I came to Uppsala, it was in October 2012. At the beginning, everything was new to me, I had no acquaintances in Uppsala and knew nothing in the field of wood science at that time. During the four–year stay in Uppsala, I have met and worked with many people, it is a pleasure to convey my gratitude to them all.

I would like to express my sincere gratitude to Professor Nasko Terziev, Professor Geoffrey Daniel and Dr. Mohamed Jebrane for their great supervision and guidance. I thank them from bottom of my heart for their great patience and continuous support, not only in my study and also in my life. I also gratefully acknowledge Cecilia Åstrand, Dinesh Fernando, Gunilla Barmark, Gabriella Danielsson, Hasanthi Karunasekera, Jie Gao, and Jongsik Kim at our department for their constant support, encouragement and inspiration. They spent a lot of time answering my scientific questions and helping with my personal issues. I learned a lot by working with them during my four years stay at our department.

Finally, I would like express my special thanks to my family, especially my wife Beini Wang. Without their love, support and encouragement, I would not be able to come to Sweden and pursue doctoral study at SLU.

Uppsala, October, 2016